

NOVEMBER 2022

IN COMPLIANCE™

THE COMPLIANCE INFORMATION RESOURCE FOR ELECTRICAL ENGINEERS

Energy Release Quantification for

Li-Ion Battery Failures

PLUS

Tailoring Safety Into
Audio Frequency Power-Line
Susceptibility Testing

South Korea Standard
KS C 9814-1:2022

Health Monitoring and
Prediction of Cells in a
Battery Module or Pack
Under Operating Condition

All you need in one small package



Antennas | Probes | Accessories | Preamplifiers | Low-Loss Cables | Recalibration Services



Travel Made Easy

with Next-Day,
On-Time
Delivery



Don't Leave home without it. A.H. Systems provides many models of Portable Antenna Kits, each containing all the necessary Antennas, Current Probes, and Cables to satisfy numerous customer requirements. Excellent performance, portability (compact size and lightweight), along with ease of setup make all of the Antenna Kits your choice for indoor or field testing. Loss and breakage are virtually eliminated as each component has a specific storage compartment within the case. All Antenna Kits are accompanied with a Tripod and Azimuth & Elevation Head, both contained in a

ANTENNAS... Tripod Carrying Case...and dont forget your keys! **and KITS TOO...**



Innovation

Quality

Performance

Phone: (818)998-0223 ♦ Fax (818)998-6892
<http://www.AHSystems.com>

A.H. Systems



Solid-State Amplifier Selection Tips for EMC Testing

Investigate the following parameters when selecting a solid-state amplifier for EMC testing:

Class of Operation

Class A solid state amplifiers are the preferred technology for EMC RI and CI testing. They are favored for repeatability of test results compared to Class AB and other types. Verify that the Class A amplifier can tolerate load mismatches and simultaneously remain operational, without amplifier damage, foldback or shutdown.

Rated Output Power

Compare actual production power curve test results, and avoid assuming rated power based on model data sheet specifications.

Linearity & Harmonic Distortion

For repeatability of test results, seek amplifiers with good linearity and low harmonic distortion. Linearity should be less than ± 1 dB (subject to your application) and harmonics are preferred below 18 dBc.

Modulation (AM, FM, PM) Performance

Modulation of CW signal is required by RI and CI test standards. Confirm that an amplifier can reproduce modulation satisfactorily to your unique application requirements.

To know more, talk to an AR applications engineer at [800.933.8181](tel:800.933.8181). AR offers over 100 amplifier models ranging from 10 kHz – 50 GHz with power levels of 1 W – 100 kW to meet your unique requirements. And as with all amplifiers from AR, these are Built to Last

Also visit us at www.arworld.us.



IN COMPLIANCE

ELECTRONIC DESIGN, TESTING & STANDARDS

AT WORK.
AT HOME.
ON THE GO.

**In Compliance
is here for you.**

[HTTPS://INCOMPLIANCEMAG.COM](https://incompliancemag.com)

In Compliance Magazine

ISSN 1948-8254 (print)

ISSN 1948-8262 (online)

is published by

IN COMPLIANCE

© Copyright 2022 Same Page Publishing, Inc.
all rights reserved

Same Page Publishing Inc.

451 King Street, #458

Littleton, MA 01460

tel: (978) 486-4684

fax: (978) 486-4691

Contents may not be reproduced in any form
without the prior consent of the publisher.

While every attempt is made to provide accurate
information, neither the publisher nor the authors
accept any liability for errors or omissions.

**editor/
publisher** Lorie Nichols
lorie.nichols@incompliancemag.com
(978) 873-7777

**business
development
director** Sharon Smith
sharon.smith@incompliancemag.com
(978) 873-7722

**production
director** Erin C. Feeney
erin.feeney@incompliancemag.com
(978) 873-7756

**marketing
director** Ashleigh O'Connor
ashleigh.oconnor@incompliancemag.com
(978) 873-7788

**circulation
director** Alexis Evangelous
alexis.evangelous@incompliancemag.com
(978) 486-4684

**features
editor** William von Achen
bill.vonachen@incompliancemag.com
(978) 486-4684

senior contributors	Bruce Archambeault bruce@brucearch.com	Ken Javor ken.javor@emcompliance.com
	Keith Armstrong keith.armstrong@ cherryclough.com	Ken Ross kenrossesq@gmail.com
	Leonard Eisner Leo@EisnerSafety.com	Werner Schaefer wernerschaefer@comcast.net
	Daryl Gerke dgerke@emiguru.com	

columns contributors	EMC Concepts Explained Bogdan Adamczyk adamczyk@gvsu.edu	Hot Topics in ESD EOS/ESD Association, Inc info@esda.org
---------------------------------	--	--

On Your Mark
Erin Earley
earley@clarionsafety.com

advertising For information about advertising contact
Sharon Smith at sharon.smith@incompliancemag.com.

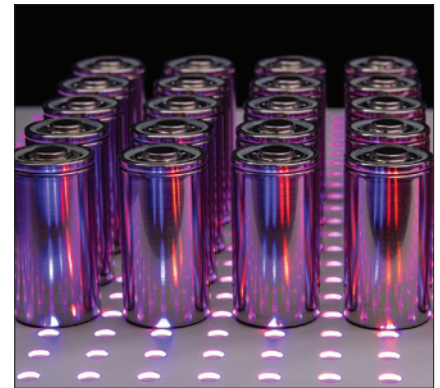
subscriptions In Compliance Magazine subscriptions are
free to qualified subscribers in North America.
Subscriptions outside North America are \$129
for 12 issues. The digital edition is free.
Please contact our circulation department at
circulation@incompliancemag.com



8 ENERGY RELEASE QUANTIFICATION FOR LI-ION BATTERY FAILURES

By Francesco Colella, Sergio Mendoza, Michael Barry, Artyom Kossolapov, Ryan Spray, and Timothy Myers

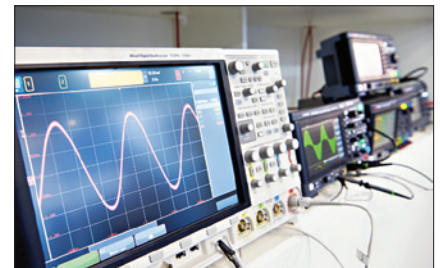
The growing application of lithium-ion batteries brings with it an increased risk of unanticipated energy releases and thermal runaway. Quantifying battery energy release characteristics during product design can help mitigate those risks.



20 Tailoring Safety Into Audio Frequency Power-Line Susceptibility Testing

By Ken Javor

Solar Electronics founder Al Parker used to say about EMI testing, "There's more than one way to skin a cat." Here are a couple more.



28 South Korea KS C 9814-1:2022 Standard

By Grace Lin

This article addresses the latest changes to the KS C 9814-1 (and CISPR 14-1) standard.



34 Health Monitoring and Prediction of Cells in a Battery Module or Pack Under Operating Condition

By Benjamin Chen

The state of health of cells in a battery pack under operating condition is difficult to obtain through existing IEC and ISO standard methods under laboratory conditions. However, a cell state of health (SOH) profile shall be able to establish by the comparison of electro-impedance spectroscopy (EIS) generated statically versus dynamic operating data retrieved by battery management system (BMS) communication interface as fragments of EIS.



6 Compliance News

45 Product Showcase

50 Advertiser Index

38 EMC Concepts Explained

46 On Your Mark

50 Upcoming Events

42 Hot Topics in ESD

48 Banana Skins

FBI Recommends Actions to **Protect Medical Devices from Cyberattacks**

The U.S. Federal Bureau of Investigation (FBI) has issued a report detailing the potential cybersecurity risks associated with outdated and unpatched medical devices.

The report, titled “Unpatched and Outdated Medical Devices Provide Cyber Attack Opportunities,” offers frightening details regarding the extent of the medical device cyber risk. For example, according to research published in 2022 and cited by the FBI, 53% of connected medical devices used in hospital settings had known, critical vulnerabilities that can pose a risk to patients, including those with severe medical conditions.

A separate 2021 research report cited in the Bureau’s report determined that the average medical device has more than six separate vulnerabilities and that medical devices at their end-of-life stage have few or no security patches or upgrades available.

The FBI’s report also provides a comprehensive list of steps that healthcare institutions can take to secure medical devices, including more robust endpoint protection, vulnerability management, and increased employee training to help mitigate risks.

EU Commission Updates **Standards for ATEX Directive**

The Commission of the European Union (EU) has published an updated list of harmonized standards that can be used to demonstrate conformity with the essential requirements of its directive concerning equipment and protective systems intended for use in potentially explosive atmospheres (2014/34/EU), also known as the ATEX Directive.

The ATEX Directive applies to “machines, apparatus, fixed or mobile devices, control components and instrumentation...and detection or prevention systems which...are intended for the generation, transfer, storage, measurement, control and conversion of energy and/or the processing of material,” and “which are capable of causing an explosion through their own potential sources of ignition.”

The updates to the list of harmonized standards under the ATEX Directive were enacted under the scope of Commission Implementing Decision (EU) 2022/1668, published in the Official Journal of the European Union in late September. The new list represents the first updates to the ATEX harmonized standards list since 2018.

FCC Expands List of **Communications Equipment That Poses National Security Threat**

The U.S. Federal Communications Commission (FCC) has moved to expand the list of communications equipment and services that pose a potential threat to U.S. national security.

According to a Public Notice issued by the FCC’s Public Safety and Homeland Security Bureau, the FCC has added products and services from two additional entities, Pacific Network Corporation and its subsidiary Com Net (USA) LLC and China Unicom (Americas) Operations Limited, to its list of companies whose equipment and services have been deemed a security threat. The FCC says that these entities “are subject to the exploitation, influence, and control of the Chinese government,” thereby posing “an unacceptable risk to the national security of the United States or the security and safety of United States persons.”

The FCC is required under the Secured and Trusted Communications Act to publish and maintain a list of communications equipment and services that pose a security risk.



You Can't Make This Stuff Up: 2022 Ig Nobel Prizes Announced

Once again, we're pleased to announce the winners of the 32nd First Annual (not a typo!) Ig Nobel Prizes. This year's awards ceremony was held virtually on and live streamed globally. The ten new Ig Nobel Prize award winners include:

- For applied cardiology, a team of researchers from the Czech Republic for research that confirmed that, when new romantic partners meet for the first time and are attracted to each other, their heart rates synchronize;
- For literature, researchers in Canada, the U.S., the UK, and Australia for confirming that poor writing and not specialized concepts are what makes legal documents unnecessarily difficult to understand;
- For biology, a pair of researchers from Brazil and Columbia on whether and how constipation affects the mating prospects of scorpions;
- For medicine, a team of researchers from Poland for demonstrating that when patients undergo some

forms of toxic chemotherapy, they suffer fewer harmful side effects when ice cream replaces one component of the procedure;

- For engineering, Japanese researchers who worked to discover the most efficient way for people to use their fingers when turning a knob; and finally...
- For peace, an international consortium of researchers who developed an algorithm to help gossipers decide when to tell the truth and when to lie.

For those who have never heard of the Ig Nobel Prizes (and, if so, where have you been?), they are not to be confused with the annual Nobel Prizes typically announced in early October in Oslo, Norway. Instead, the Ig Nobel Prizes "honor achievements that first make people laugh and then make them think."



Your One-Stop Product Safety Shop – Everything You Need for Product Safety!

ED&D

PRODUCT SAFETY SOLUTIONS

www.ProductSafeT.com

IEC/ISO 17025 Accredited Calibrations

Equipment Calibrated in **SCOPE!**

ED&D is the worlds leading source for precision product safety test equipment. Our engineers are the most qualified in the industry. We'll show you how to save time & money in the regulatory process. Test in advance to be sure you pass the first time!

Call Us Today!
 USA/Canada Toll Free:
800.806.6236
 International:
+1.919.469.9434
 Website:
www.ProductSafeT.com
 Research Triangle Park • North Carolina • USA



Force Gauges

**Save Time...
 Save Money...
 Get Smart...**

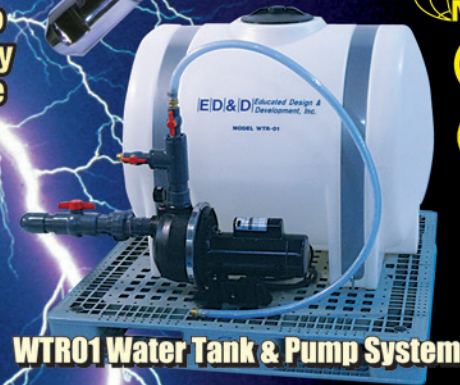
Finger Probes



Impact Hammers



JET-01 & JET-02 Jet Nozzles

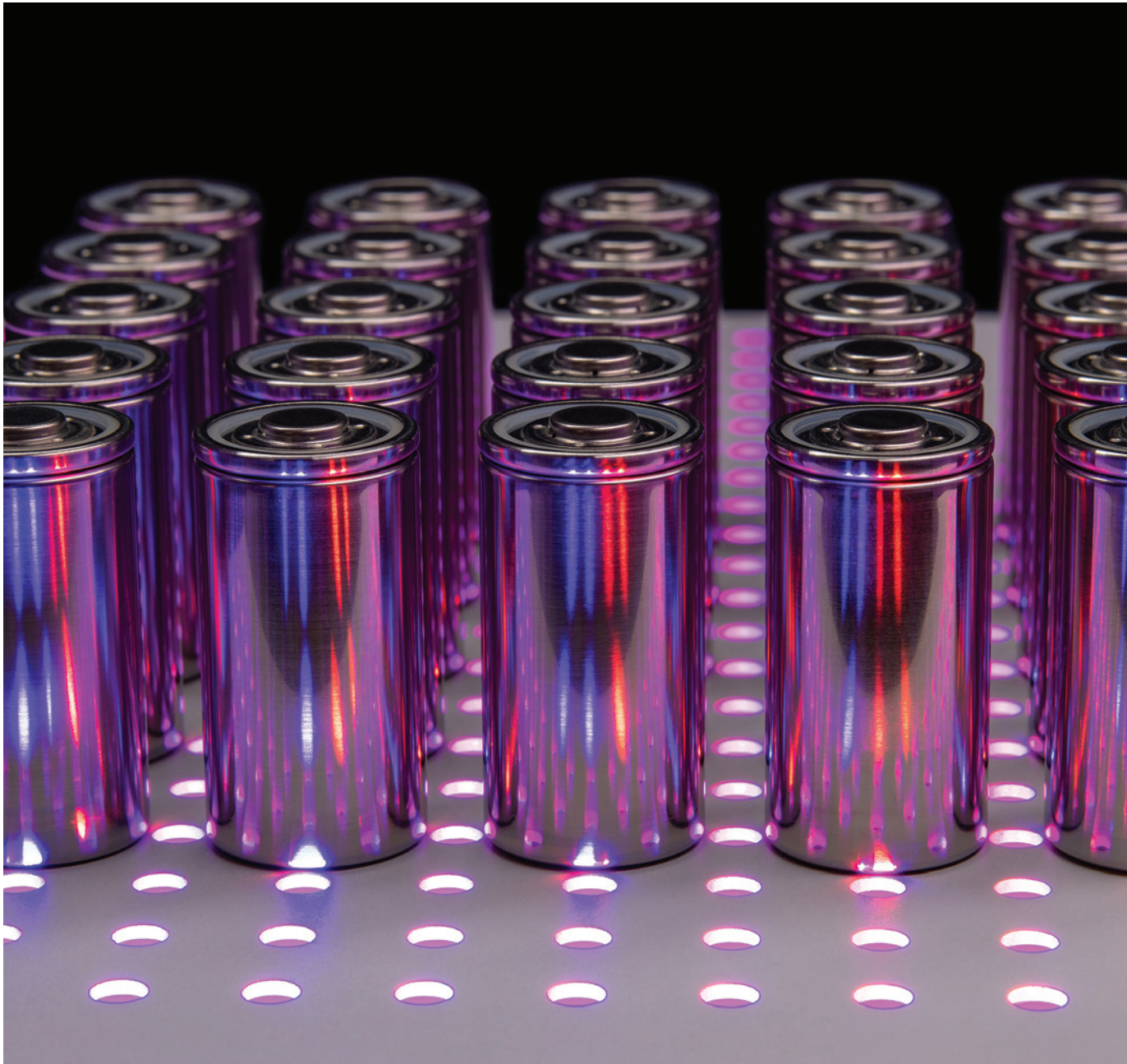


WTR01 Water Tank & Pump System



ENERGY RELEASE QUANTIFICATION FOR LI-ION BATTERY FAILURES

Evaluation and Testing Can Reduce Battery-Related Safety Risks



By Francesco Colella, Sergio Mendoza, Michael Barry, Artyom Kossolapov, Ryan Spray, and Timothy Myers

This article presents an experimental framework to characterize the energy released during thermal runaway events involving Li-ion cells and battery packs used in applications ranging from electric vehicles to consumer electronics and medical devices to aerospace applications. A brief introduction to lithium-ion batteries and battery thermal runaway is provided. The article then describes various methods for obtaining energy release in cells undergoing thermal runaway.

The first method involves testing a cell inside a sealed pressure vessel, which allows for the estimation of the volume of gas produced as a result of thermal runaway and a quantitative assessment of the vent gas composition. This technique is generally used to assess the flammability hazards associated with thermal runaway. The second method described is oxygen consumption calorimetry. This technique provides an estimation of the heat released by a cell undergoing thermal runaway via chemical analysis (i.e., how much oxygen has been consumed and the associated heat release).

The third and fourth methods include two techniques designed to estimate the energy yielded during a battery thermal runaway event: the accelerating rate calorimetry (ARC) and a novel methodology designed to estimate the sensible energy released during a

battery thermal runaway failure using a fractional thermal runaway calorimeter (FTRC) apparatus.

THE GROWING RISK OF LI-ION BATTERY FAILURES

Over the last ten years, lithium-ion (Li-ion) batteries have become the energy storage technology of choice for different industries, including automotive, consumer electronics, and aerospace applications. As Li-ion battery chemistries improve, battery energy and power densities have increased. Increasing energy densities, including implementation of lithium-metal-containing cells, result in higher potential risks and/or severity of battery failure events. The increased risk stems from both the presence of higher amounts of energy and thinner, tighter tolerances of internal components.

One catastrophic failure mechanism that can lead to battery fires is a thermal runaway event. In large, multi-cell packs such as those commonly used in electric vehicles or stationary energy storage systems, the heat generated by one failed cell can heat up neighboring cells which may lead to a thermal cascade throughout the battery pack. It is generally expected that there will occasionally be single cell failures within a population of lithium-ion battery packs. This potential for propagation of failures presents an increased risk to property and safety.



Francesco Colella is a Senior Managing Engineer in Exponent's Thermal Sciences practice and can be reached at fcolella@exponent.com.



Sergio Mendoza specializes in battery model-based control, estimation, information theory, and experiment design.



Michael Barry specializes in assessing mechanical and thermal failures in a wide range of products and systems.



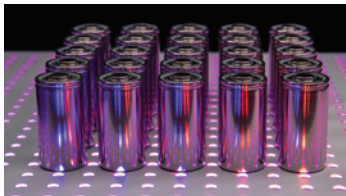
Artyom Kossolapov has expertise in heat transfer, fluid mechanics, multiphase flow, and thermal hydraulics of nuclear reactors.



Ryan Spray is a Principal Scientist in Exponent's Polymer Science & Materials Chemistry practice.



Timothy Myers is a principal engineer and director of the Exponent, Inc. Natick, MA office.



One reason for the concern over the propagation of failures is that thermal runaway events can result in the venting of flammable gases, and these gases can generate a fire or an overpressure event if ignited in a confined area.

Underwriters Laboratories (UL) recently created a new test method (UL 9540A, Test Method for Evaluating Thermal Runaway Fire Propagation in Battery Energy Storage Systems) that specifically seeks to assess the propensity of energy storage systems to exhibit propagating failures. One reason for the concern over the propagation of failures is that thermal runaway events can result in the venting of flammable gases, and these gases can generate a fire or an overpressure event if ignited in a confined area. Multiple failures occurring due to propagation will subsequently release a larger volume of flammable gases.

An accurate evaluation of the energy yielded during a battery thermal runaway failure is of critical importance for the design of any battery-powered product from both safety and performance standpoints. Accurate energy yield estimates are valuable for a large variety of tasks, including but not limited to:

- Comparisons of failure characteristics of batteries from different formats and vendors;
- Evaluation of the ultimate fate of the energy released (i.e., is the heat released contained within the vented gases or in the cell body);
- Design of safer battery packs that minimize the likelihood of cascading failure events involving neighboring cells; and
- Create reliable inputs for mechanical or thermal models of devices or battery packs.

The energy released during a battery thermal runaway failure can roughly be assessed by evaluating the sensible energy and chemical energy components that evolved during the event. The sensible energy components can be evaluated by estimating the amount of energy required to increase the temperature of the cell body, gases, and ejecta to the levels experienced during a thermal runaway failure (prior to any combustion event occurring).

The chemical energy component can be assessed by estimating the energy released by the combustion of the vent gases following their release from the cell body during the thermal runaway event. The characterization of the combustion energy requires a characterization of the composition and amounts of vent gases released during the failure event.

The following sections provide an overview of a battery thermal runaway failure as well as a number of techniques that can be used to characterize the energy yielded during a battery failure and its components.

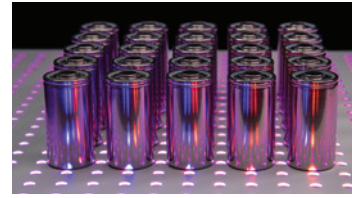
BATTERY THERMAL RUNAWAY

Thermal runaway occurs when the internal temperature of a cell increases in an uncontrolled manner, leading to its failure. In the first phase of thermal runaway, the solid electrode interface (SEI) layer decomposes in an exothermic reaction. This is followed by an exothermic reaction between the intercalated Li ions and the electrolyte. As the positive electrode materials react with the electrolyte, oxygen is evolved inside the cell, the electrolyte decomposes, and the cell disintegrates. During the thermal degradation of the Li-ion cell, the temperature increase generates gases, which are released through pressure relief vents when the pressure inside the cell rises above a design relief pressure or if the cell's enclosure fails. For Li-ion cells, these gases are hot and combustible, which can become a hazard if a pack was not designed to control the causes and consequences of thermal runaway.

All thermal runaway events are a result of a rise in cell temperature. This temperature rise can be due to multiple causes, including but not limited to:

- External heating from a high ambient temperature, thermal abuse, or external fire;
- A defect inside the cell that results in an internal short circuit, which causes the cell to heat up at the location of the defect;

During a thermal runaway event, the cell produces gases that build up within the cell. Some cell designs (e.g., cylindrical cells) include one or more designed vents that open to release the gases.



- A surge in the charging or discharging current. When cells are charged or discharged, heat is generated. The higher the current, the higher the heat generation;
- An improper electrical connection at the tab of a battery. This causes an increased electrical resistance which generates heat at the electrical contacts;
- Mechanical damage to the cell or battery that can also lead to internal shorts and result in heat generation.

During a thermal runaway event, the cell produces gases that build up within the cell. Some cell designs (e.g., cylindrical cells) include one or more designed vents that open to release the gases. In some cases, these vents can become obstructed or may not be able to adequately vent gases, which may result in rupture of the cell enclosure. Other cell form factors, such as pouch cells, often do not include a specific vent and the gases will release at weak points in the external pouch, typically near the tabs of the cell or along the pouch seams in unconstrained cells.



OUR EMC TEST SOLUTIONS

CONDUCTED IMMUNITY TESTING



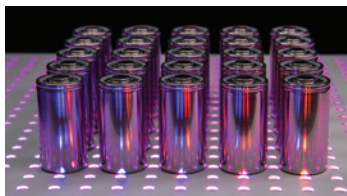
ESD3000

- › Electrostatic Discharge Testing
- › IEC 61000-6-2 and many more standards
- › Wide range of networks for specific applications
- › Up to 30kV air and contact discharges
- › Up to 3 test tips included
- › Battery charger & firmware update available
- › Rechargeable long-life batteries



IMU Series

- › Burst up to 8kV / Surge & Ring wave up to 8kV
- › One touch edit in run mode
- › Multi touch graphical interface
- › Select report format for test data
- › Integrated CDN up to 300V / 16A



Vent gas composition, flammability characteristics, and potential combustion energy released in the event of ignition can be evaluated by forcing a cell failure in a sealed vessel testing apparatus.

SEALED VESSEL TESTING

Vent gas composition, flammability characteristics, and potential combustion energy released in the event of ignition can be evaluated by forcing a cell failure in a sealed vessel testing apparatus. The sealed vessel is designed to contain the battery vent gases and to quantify the vent gas volume by tracking the temperature and pressure increase in the vessel. The sealed vessel testing apparatus includes a sampling port through which the vented gases can be collected in a sample canister and analyzed for composition using techniques such as gas chromatography (GC) and gas chromatography-mass spectrometry (GC-MS). Note that depending on the cell capacity, different sealed vessel sizes need to be used depending on the expected vented gas volume. Figure 1 shows a photograph of a 60-liter sealed vessel connected to a 20-liter combustion chamber used for battery vent gas explosion testing.

We previously produced a paper outlining the methodology for this type of testing [3]. The results presented were relative to small format Li-ion pouch cells (7.7 Wh nominal, 2.1 Ah, 3.7 V) even though both the testing and analytical methods presented could be similarly applied to larger format cells. The cells consisted of a negative electrode with graphite active material and a positive electrode with LiCoO_2 active material. Note that cell chemistry, cell geometry, ambient atmosphere, as well as the way the thermal runaway process is initiated all influence the quantitative behavior of the failure.

Table 1 summarizes the amount of gas vented during a thermal runaway event for pouch cells at three different states of charge (a more detailed description can be found in [1]). For comparison, the volume reported is referenced to standard pressure and temperature. It should be noted that for large battery packs, the amount of gas that is released can be substantial.

Table 1 and Table 2 show (1) the vent gas volume as a function of the cell SOC, and (2) the gas composition for different SOCs, respectively. With the exception of carbon dioxide, all the substances reported in Table 2 are flammable. In addition, carbon monoxide and some of the hydrocarbons are not only flammable but can also pose significant health hazards.

Note that Table 2 summarizes the species volume fraction of the vent gases. The absolute volume of each species depends on the total volume of gas vented, which increases as the SOC increases. Therefore, the total volume of hydrogen released from a 150% SOC cell is significantly higher than from a 50% SOC cell, despite having similar hydrogen volume fractions.

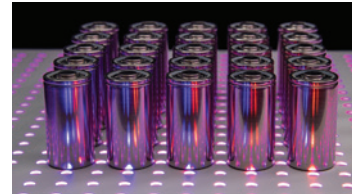


Figure 1: Photograph of a 60-liter sealed vessel connected to a 20-liter combustion chamber for battery vent gas explosion testing

State of Charge	Vented Gas Volume	Volume per Wh
50%	0.8 L / 0.2 Gal	0.10 L/Wh
100%	2.5 L / 0.7 Gal	0.33 L/Wh
150%	6.0 L / 1.6 Gal	0.78 L/Wh

Table 1: Venting gas volumes for a 7.7 Wh pouch cell at standard pressure and temperature. As a comparison, the cell has a volume of 0.014 L.

Another point to note is that the gases vented from Li-ion cell failures have a broader combustion range than typical hydrocarbons increasing the potential for ignition (likely due to the presence of hydrogen).



The combustion characteristics of the vented gases are summarized in Table 3 and compared with those of common gases. The combustion properties of the vented gases are similar to typical hydrocarbons despite the large presence of carbon dioxide. Another point to note is that the gases vented from Li-ion cell failures have a broader combustion range than typical hydrocarbons increasing the potential for ignition (likely due to the presence of hydrogen). More information on the testing methodology to evaluate the explosibility characteristics of battery vent gas is available in [1,2].

OXYGEN CONSUMPTION CALORIMETRY

Oxygen consumption calorimetry has been used for many years used to estimate the heat released during the combustion of fabrics or other typical organic materials. The established technique has found new relevance with respect to battery heat release assessments. In an oxygen consumption calorimeter, a sample usually reaches ignition and burns after being subjected to external heating. The energy released during combustion and the volume of combustion products are determined by collecting and analyzing the oxygen, carbon dioxide, and carbon monoxide contents of the exhaust gases.

The standard method by which the cone calorimeter results are processed is sometimes modified to account for the complex composition

of a Li-ion cell. A detailed description of the challenges associated with performing calorimetry of Li-ion cells is discussed in [5]. Often, the combustion event does not only involve the combustion of the

Gas		50% SOC (%vol)	100% SOC (%vol)	150% SOC (%vol)
Carbon Dioxide		32.3	30.0	20.9
Carbon Monoxide		3.61	22.9	24.5
Hydrogen		31.0	27.7	29.7
Hydrocarbons	Methane	5.78	6.39	8.21
	Ethylene	5.57	2.19	10.8
	Ethane	2.75	1.16	1.32
	Propylene	8.16	4.52	0.013
	Propane	0.68	0.26	2.54
	Isobutane	0.41	0.20	0.13
	n-Butane	0.67	0.56	0.39
	Butenes	2.55	1.58	0.60
	Isopentane	0.45	0.07	0.036
	n-Pentane	1.94	0.73	0.30
	Hexanes +	4.94	2.32	8.21
	Benzene	0.14	0.11	0.33
	Toluene	0.061	0.018	0.052
Ethyl-benzene	0.009	0.002	0.003	

Table 2: Vented gas composition for a 7.7 Wh pouch cell [3]

Gas	LFL	UFL	P _{max} (barg)	K _g (m-bar/s)
Li-Ion Vent Gas (100% SOC)	6%	~38%	7.1	65
Li-Ion Vent Gas (150% SOC)	6%	40%	7.7	90
Methane	5%	15%	6.7	46
Propane	2%	10%	7.2	76
Ethane	3%	12%	8.0	171
Hydrogen	4%	75%	6.5	250

Table 3: Combustion characteristics of vented gases released during a thermal failure of 7.7 Wh cells, and of common gases [4]

vented gases, but solid components of the cell itself also burn and release energy.

To quantify the amount of energy that can be released by a cell involved in a fire, small format Li-ion pouch cells (7.7 Wh nominal, 2.1 Ah, 3.7 V) were tested in a cone calorimeter. Evolutions of gases released, oxygen consumed, and mass loss from the combustion reaction of the Li-ion cell charged at 50% SOC are presented in Figure 2. Figure 2a. shows an initial increase in production rates of CO₂ and CO concurrent with an initial mass loss of cell material (Figure 2c.) for about 15 seconds, starting at approximately 50 seconds. This phase corresponds to the ignition of the vented gases. The release of combustion gases is combined with an initial increase in oxygen consumption as shown in Figure 2b. During this period, the bulk material within the Li-ion cell is not involved in the combustion reaction. Electrolyte vapors are most likely the major contributor to the combustion during this 1st phase.

After the 1st phase, a transition to faster reaction kinetics is observed at approximately 65 seconds. Increases in the CO₂ and CO production rates combined with a rise in oxygen consumption are shown on Figure 2a., 2b., and 2c. This large increase is confirmed by changes in the slope of the production, consumption, and mass loss rate curves. At this stage, the bulk material within the cell is involved in the combustion process. This 2nd phase lasts for approximately 35 seconds before extinction occurs. The peaks of CO₂ and CO are respectively 1.3 and 0.02 g/s. The total mass loss at the end of the test is about 8.4 g. This mass loss compares to the total mass of organic compounds present in the Li-ion cell and is evaluated to be approximately 9.0 g.

Although the cone calorimeter can be used to determine several parameters (e.g., critical heat flux for ignition, ignition time, etc.), one of the most important parameters measured is the heat release rate (HRR). The HRR is the amount of energy produced by the combustion process per unit of time (expressed typically in kW). It is the single most important parameter for determining the fire hazards associated with a given material

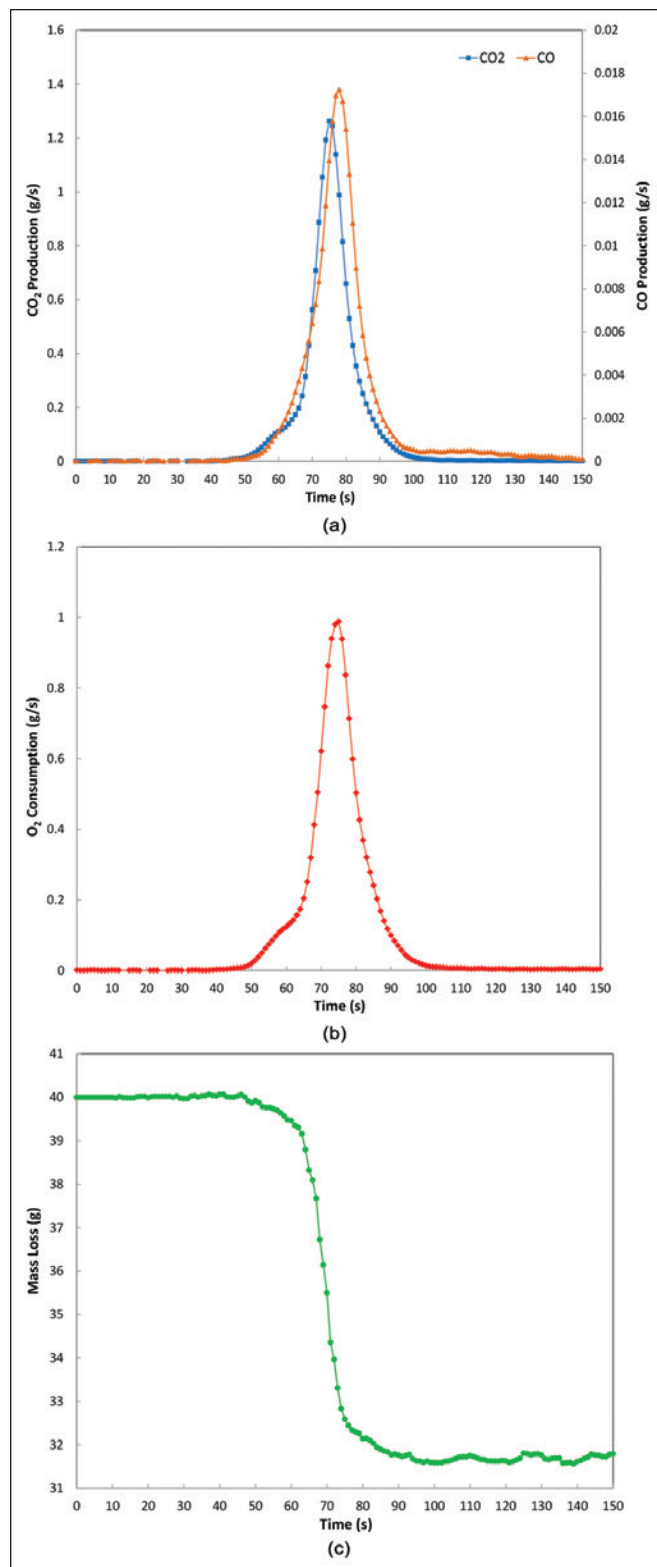


Figure 2: (a) CO₂ and CO production rates, (b) O₂ consumption rate, and (c) mass loss from the combustion of Li-ion cell charged at 50% SOC

or product and for designing fire protection systems. Figure 3 shows the evolution of the heat release rate as a function of time for a 7.7 Wh Li-ion cell at 0%, 50%, and 100% SOC. At the peak of the combustion event, the fire releases approximately 22 kW, 13 kW, and 2 kW of power for cell SOC's equal to 100%, 50%, and 0%, respectively. Once again, the heat release rate is very dependent on the state of charge of the cell.

ACCELERATING RATE CALORIMETRY (ARC)

An accelerating rate calorimeter (ARC) is an instrument designed to characterize the self-heating behavior of materials and reaction kinetics that in recent years, has become highly utilized to understand the thermal runaway processes of batteries.

In ARC testing of batteries, the protocol typically follows a heat-wait-search (HWS) algorithm that minimizes heat losses from the sample to the surroundings. More specifically, the ARC system and sample are first heated to a set temperature point and are independently monitored for temperature. Both are then allowed to wait to equilibrate temperatures for a set amount of time, before actively searching for temperature rise from the sample. If no sample self-heating is detected, the system moves to

the next temperature step, typically 5 °C or 10 °C, and begins the H-W-S process again.

Once the system detects self-heating of the sample during a search step, the system increases its temperature to match the sample temperature, thus creating an adiabatic environment. This temperature tracking continues until the cell thermally fails or a designated temperature set point is reached. Evaluating the self-heating as a function of temperature, cell voltage, and sometimes the evolved gas/pressure for ARC tests in a sealed vessel allows for analysis of various chemical reactions and events that

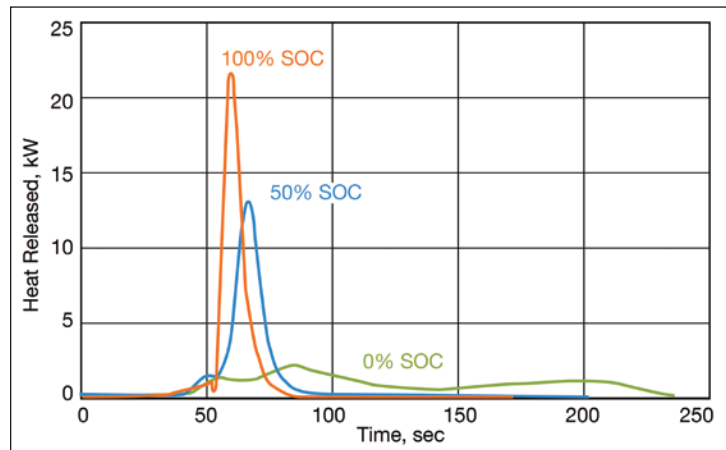


Figure 3: Heat release rate (HRR) during the combustion of a 7.7 Wh Li-ion cell at 0%, 50%, and 100% SOC

Cx Family Power Line Common Mode Chokes

- Solutions for use in a wide array of power line circuits
- Suppress high frequency common mode noise up to 100 MHz
- 1000/1500 Vrms isolation and up to 10 Amps Irms
- Low-profile, toroidal construction

Coilcraft



Free Samples @ coilcraft.com

occur during thermal failure of a cell. These include solid electrolyte interface (SEI) decomposition, electrolyte venting from cell enclosures, separator failure and/or shut-down, positive electrode oxidation, and more (see Figure 4).

ARC can be used to study the variety of variables that affect the thermal decomposition and runaway characteristics, including cell size/shape/capacity, cell format, SOC (see Figure 5), chemistry and morphology of the electrodes, electrolyte composition, state-of-health (or life), presence of plated lithium metal, etc. If ARC testing is performed with the battery sample in a sealed vessel (e.g., inside of the larger ARC chamber), the overall energy release from the thermal runaway event can be estimated using the heat capacity of the sample in conjunction with the temperature rise experienced on the sample, the temperature rise of the ARC vessel, and the known heat input into the system via recorded heater power.

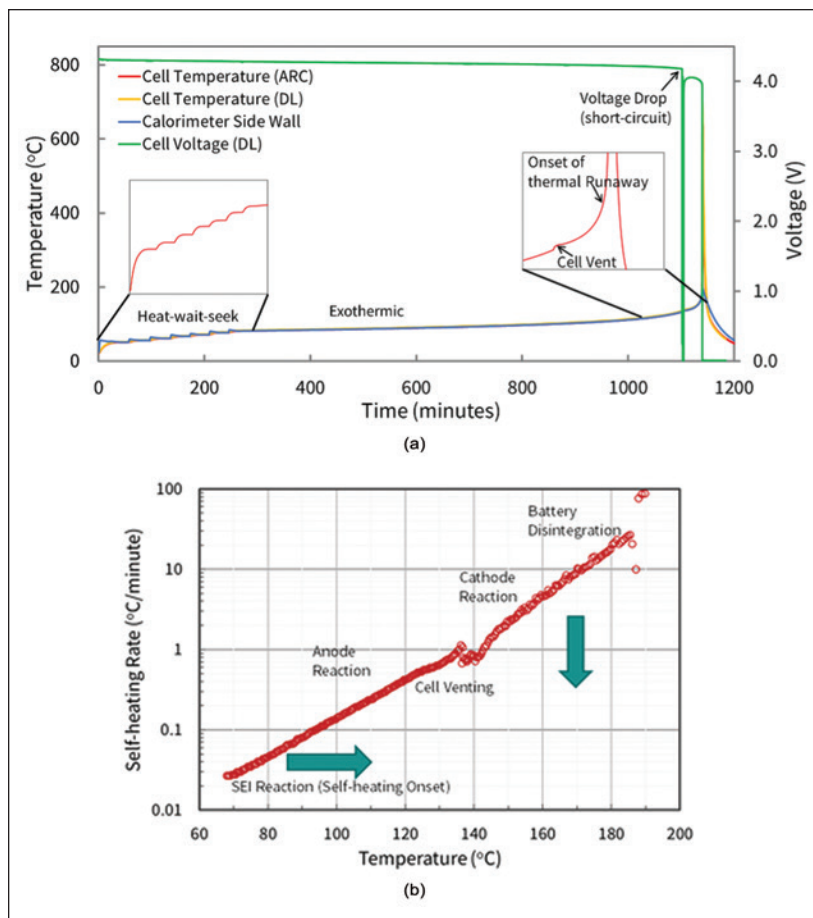


Figure 4: Accelerating rate calorimetry data showing (left) heat-wait-search program testing of a charged lithium-ion battery and (right) a self-heating rate vs. temperature plot identifying characteristic features in the battery failure

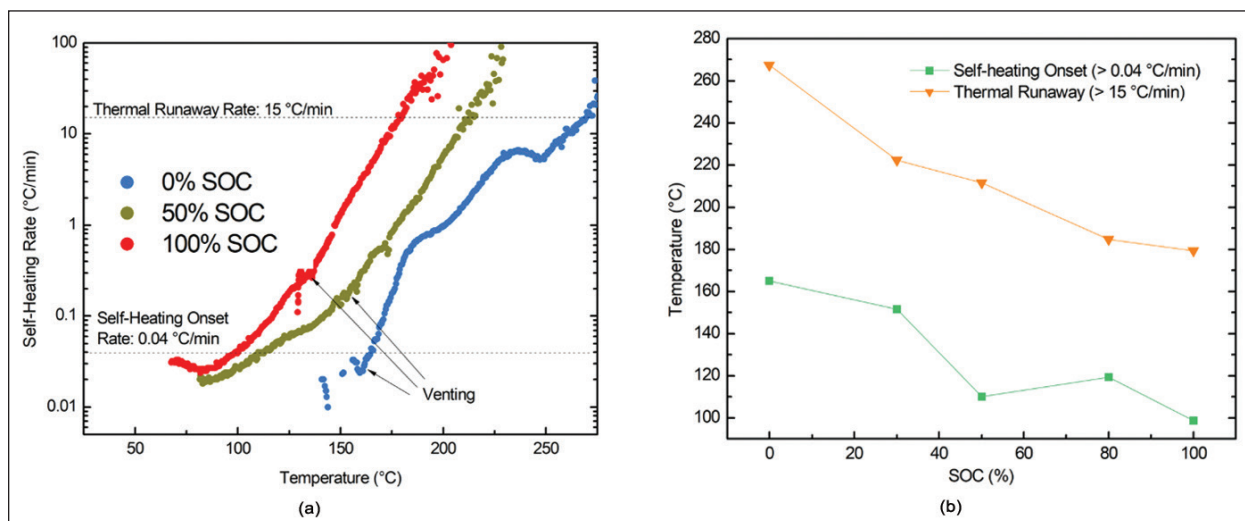


Figure 5: ARC analysis of 18650-format lithium-ion cells at various SOC showing a decrease in the self-heating onset and thermal runaway temperatures with an increase in SOC

FRACTIONAL THERMAL RUNAWAY CALORIMETER

A fractional thermal runaway calorimeter (FTRC) is a battery testing apparatus specifically designed by the National Aeronautics and Space Administration (NASA) to measure the energy output and mass ejections associated with a battery thermal runaway event [6]. The FTRC is equipped with interchangeable cell chambers that can accommodate cells with various form factors and capacity (i.e., 18650 cells, 21700 cells, D cells) as well as different cell triggering mechanisms ranging from external heating to nail penetration and internal short circuit devices. The cell chamber is centrally located and is interfaced on either side with (1) ejecta mating assemblies, (2) ejecta bore assemblies, and (3) rod-and-baffle assemblies.

An FTRC apparatus equipped with a standard 18650 cell chamber is fundamentally a symmetric device that can evaluate energy released associated with cell failures encompassing top venting, bottom venting, or both. The operation of the FTRC rests on simple physical principles. The various assemblies of the FTRC are all composed of known materials with known masses. The temperatures of these components are recorded throughout a test run. Since the material composition of the assemblies is well known, it is known how much energy must be added to the assemblies to cause a given rise in temperature. Thus, by measuring the component temperatures, it is simple

to compute how much energy was transferred to those components (i.e., how much energy the cell released).

The cell chamber is connected to the ejecta mating assemblies via ceramic bushings that provide a certain degree of thermal isolation between the sub-assemblies while guaranteeing the continuity of the flow path for the vent gases ejected during the battery failure event. The ejecta mating assemblies are designed to capture large debris and ejecta released during cell failure. The ejecta bore assemblies and rod-and-baffles assemblies are located downstream of the ejecta mating and are designed to extract sensible energy from the vent gases by creating a tortuous flow path encompassing (1) a series of aluminum baffles and (2) copper mesh windings. Figure 6 shows a photograph of an FTRC equipped with a 18650 cell chamber. Note the two copper mesh windings prior to installation in the FTRC.

The energy evolved during the battery failure can be evaluated in terms of total energy yield, fractional energy yields associated with the battery body, and positive/negative vent gas and ejecta. The cell energy yield is obtained by solving an energy balance equation for all the sub-components of the calorimeter based on the mass, specific heat, and temperature increase experienced by each sub-assembly. More specifically, the sub-assembly temperature increase is measured by over 100 type-K thermocouples attached to the hardware of the calorimeter in multiple locations.

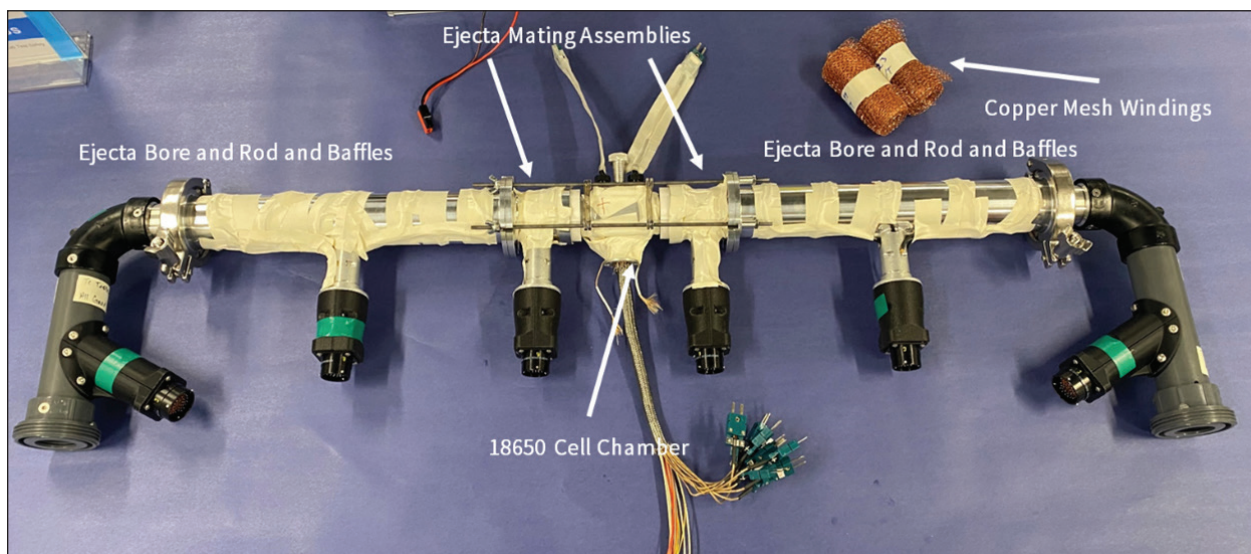


Figure 6: Photograph of an FTRC apparatus equipped with a 18650 cell chamber in the center of the device

Examples of energy yield estimations associated with battery thermal runaway events is presented in Figures 7, 8, and 9. We performed triplicate FTTC tests on 18650 cells with a capacity of 2.6 Ah and a state-of-charge of 100%. Figure 7 shows a bar plot depicting the total energy yield that evolved during a thermal runaway event of the three subject cells. The testing results show a total energy yield ranging between approximately 48 kJ and 52 kJ. The yield fractions associated with the cell body range between 26kJ and 31kJ and those associated with the positive vent gas and eject range between 19 kJ and 26 kJ. Figure 8 shows the time-dependent evolution of energy yielded by the cell failure as measured by the calorimeter apparatus. Figure 9 shows the fractional mass distribution measured during the tests.

The results show that the vast majority of the mass remains within the cell body following the thermal runaway event. Smaller mass fractions were associated with the ejecta that were accumulated along the positive side of the calorimeter (*i.e.*, in the positive ejecta mating, copper mesh, rod-and-baffles, and bore). Virtually no mass (or energy) was released towards the negative portion of the calorimeter that interfaces with the bottom of the cell.

Figure 9 also shows the amount of unrecovered mass during the experiment. Unrecovered mass is associated with the amounts of vent gases and small ejecta that can leave the apparatus during the test. It should be noted that the energy fraction associated with the unrecovered mass is generally

small. This is due to the fact that the temperature of vent gases and ejecta leaving the calorimeter is relatively close to ambient since the calorimeter is

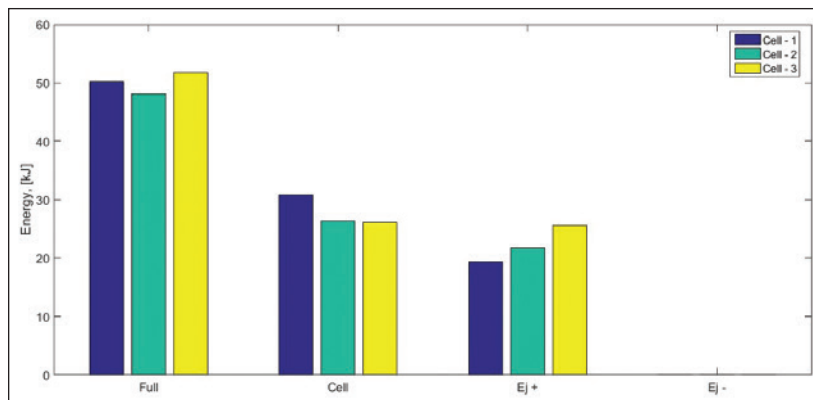


Figure 7: Bar plot showing the total energy yield during the thermal runaway event for the 3 subject 18650 cells

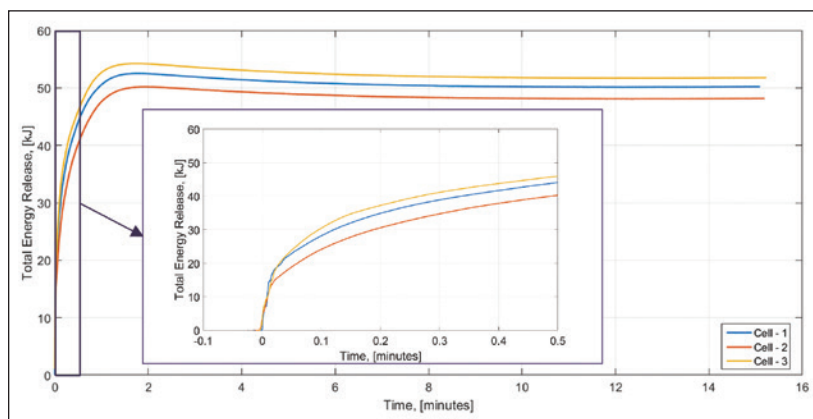


Figure 8: Time-dependent evolution of the energy evolved during the thermal runaway event for the 3 subject 18650 cells

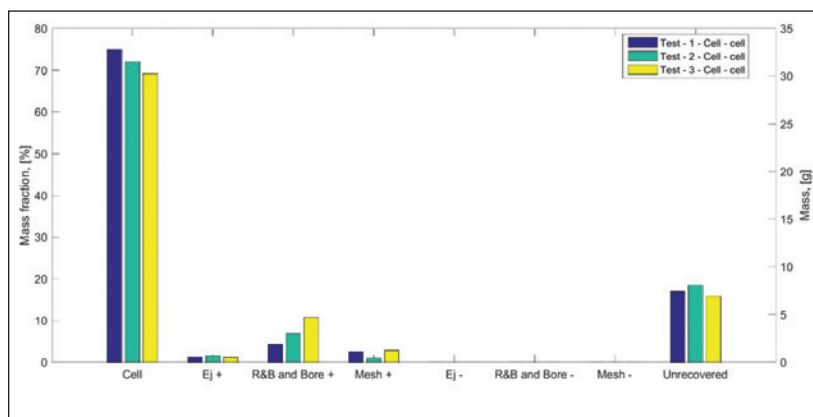


Figure 9: Fractional mass distribution associated with the thermal runaway event for the 3 subject 18650 cells

designed to extract all their sensible energy along the tortuous path leading from the cell chamber (where vent gases and eject are generated) through the rod-and-baffles assemblies and the copper mesh.

CONCLUSION

This article presents a chemistry-agnostic, experimental framework to characterize the energy released during a thermal runaway event of a lithium-ion cell. The characterization of the energy yielded during a failure is a critical parameter that can inform the design of battery-powered products from safety and performance standpoints. The framework relies on multiple experimental methodologies such as (1) sealed vessel testing, (2) oxygen consumption calorimetry testing, (3) ARC, and (4) FTRC testing. Combined, these techniques offer quite a complete picture of the energy and materials released during the thermal runaway of a lithium-ion battery. 

REFERENCES

1. Somandepalli, V, Marr, K, and Horn, Q, "Quantification of Combustion Hazards of Thermal Runaway Failures in Li-ion Batteries," *SAE International Journal of Alternative Powertrains*, 3(1):2014.
2. Colella F., Ponchaut N.F., Biteau H., Marr, K., Somandepalli V., Horn Q.C., Long, R.T., "Characterization of Electric Vehicle Fires," *Proceedings of the 16th International Symposium on Aerodynamics, Ventilation & Fire in Tunnels*, 15-17 September 2015, Seattle, WA.
3. Colella, F., Marr, K., Ponchaut, N., Somandepalli, V., Spray, R., "Analysis of Combustion Hazards due to Catastrophic Failures in Li-ion Battery Packs," *7th International Seminar on Fire and Explosion Hazards*, 5-10 May 2013, Providence, RI.
4. *The SFPE Handbook of Fire Protection Engineering, 4th Edition*, Society of Fire Protection Engineers, 2008.
5. Somandepalli, V., Biteau, H., "Cone Calorimetry as a Tool for Thermal Hazard Assessment of Li-Ion Cells," *SAE International Journal of Alternative Powertrains*, 3(2):2014.
6. Walker W., et. al. "The Effect of Cell Geometry and Trigger Method on the Risk Associated with Thermal Runaway of Lithium-ion Batteries," *Journal of Power Sources*, 524, 2022.

ISO 21498 - 2: 2021



Electrically propelled road vehicles -
Electrical specifications and tests for voltage class B
systems and components - Part 2: Electrical tests for
components

ISO 21498 E-vehicles HV Test System



- * Voltage output DC 0V ~ 1000V / 1500V; arbitrary wave editing;
- * Support system configuration upgrade; current output 60A~1000A;
- * Support superimposing ripple frequency 400kHz; ripple output 900A lpp; satisfy the test requirement of battery modules;
- * 1500V/ms voltage slew rate;
- * Simulating complex electrical environment occurred in the actual application of E-vehicles HV components and battery modules;
- * Meet the test requirement of ISO 21498-2:2021.
LV 123, VW 80300-2016, Mercedes MBN 11123.



SUZHOU 3CTEST ELECTRONIC CO., LTD.

Add: No.99 E'meishan Road, SND,
Suzhou, Jiangsu Province, China
Email: globalsales@3ctest.cn
Ph: + 86 512 6807 7192
Web: www.3c-test.com



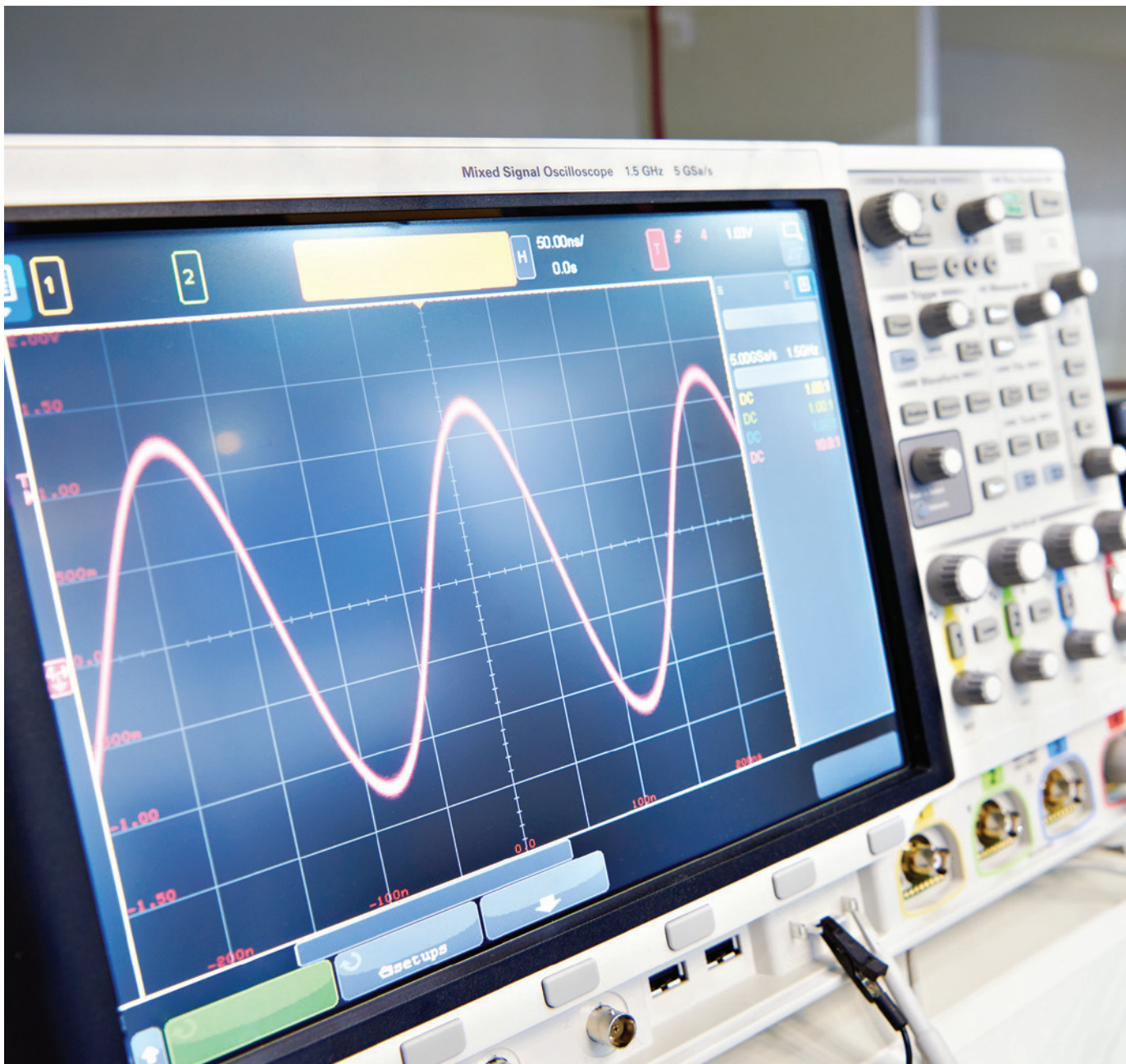
You Tube

0411200010 | 0411200011
No.01172000020001

SUBSCRIBE: 3CTEST

TECH TIP: TAILORING SAFETY INTO AUDIO FREQUENCY POWER-LINE SUSCEPTIBILITY TESTING

Some Safer Ways to Conduct Audio Frequency Conducted Susceptibility Testing



Ken Javor is a Senior Contributor to *In Compliance Magazine* and has worked in the EMC industry for over 40 years. Javor is an industry representative to the Tri-Service Working Groups that maintain MIL-STD-464 and MIL-STD-461. He can be reached at ken.javor@emccompliance.com.



By Ken Javor

Note: This technical tip assumes a basic familiarity with the injection of audio frequency ripple on equipment input electrical power in accordance with such standards as MIL-STD-461 CS01/ CS101, RTCA/DO-160 section 18, and ISO 11452-10 (preceded by SAE J 1113/2) (References 1-8).

This technical tip presents safer ways of performing audio frequency conducted susceptibility testing than the standard approach described in References 1-8. “Safer” here means reducing the probability of accidentally damaging the test article, either by over-testing, or by inducing instability in the test article’s internal switched mode power supply, or by causing a shutdown of the audio amplifier resulting in possible instability in the test article internal switched mode power supply.

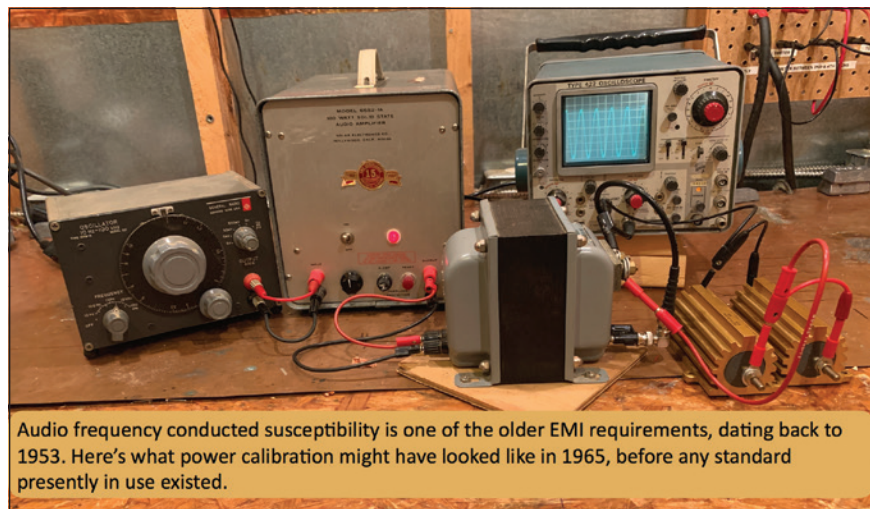
These are always important considerations, but especially so when the test article is a one-of-a-kind item whose delivery is on the program schedule critical path. Finally, the stability issue is most pronounced when the test article runs off a dc bus, because dc/dc converters tend to have much smaller hold-up capacitors out front than if the cap providing the hold-up function also has to smooth out ripple from a 50/60/400 Hz ac bus.

A prime example of a sensitive load running off a dc bus is equipment used on spacecraft and launch vehicles. Further, such may be one-of-a-kind items where the actual flight unit is being EMI qualified.

References 1-8 provide similar limits and test methods.

Spacecraft audio conducted susceptibility limits and test methods are based on various issues of MIL-STD-461/-462, References 1-5 (viz. AIAA S-121, Reference 9). As found in Reference 9, most spacecraft audio conducted susceptibility limits are tailored much lower than the limits found in any of References 3-5, for reasons described in Reference 10.

Another difference between References 1-5 and spacecraft derivatives is that the spacecraft derivatives tend to compute a power limit based on the dc voltage limit, whereas MIL-STD-461 CS01/CS101 use the power from the higher ripple limit for higher potential (ac) buses. This results in the use of amplifiers of at least 100 W output, and often 300 W or higher. Further, many such amplifiers have quite low output impedances, so that they can deliver much more than the pre-calibrated power if the input impedance of the test article dips below 0.5 Ω . To promote safety, it is advisable to use no more power than is absolutely necessary and to have an output impedance of around 2 Ω (which transforms to 0.5 Ω across the coupling transformer windings).



Audio frequency conducted susceptibility is one of the older EMI requirements, dating back to 1953. Here’s what power calibration might have looked like in 1965, before any standard presently in use existed.

Solar Electronics used to supply audio power oscillators and amplifiers with a $2.4\ \Omega$ output impedance, but they no longer sell audio sources or amplifiers. When using an amplifier with (typically) lower output impedance, additional resistance may be added in series between the amplifier output and the input to the primary side of the coupling transformer. This protects the test article from excessive input ripple current but also protects the amplifier itself from a short-circuit condition that could cause protection circuitry to trip. When an amplifier shuts down to protect itself, it can actually damage the test article because, if the primary side of the coupling transformer is open-circuited, the secondary side looks like a one millihenry inductor in series between the power source and the test article (Reference 1, page 33-34). If the test article has insufficient capacitive decoupling in front of its dc/dc converter, it can go unstable, drawing too much switched mode current through the coupling transformer secondary. This has caused damage to (space) flight hardware power supplies.

An added benefit to a series output resistor on a low output impedance amplifier is protecting that amplifier from reflected ac ripple when the test article is powered from an ac (50/60/400 cycle) power bus. If the added resistor is large with respect to the actual amplifier output impedance, most of the reflected ac ripple drops across the added resistor, not the amplifier output itself.

In this tech tip, two approaches to protecting against such problems are explored. One uses a low rather than high-power amplifier, and the other technique inserts an attenuator

between the output of a high-power amplifier and the coupling transformer primary. The attenuator prevents too much power in the event of an operator error, but also places an effective $2\ \Omega$ resistance across the primary of the transformer even if the amplifier goes open so that the test article will never see more than $0.5\ \Omega$ inserted between itself and the power source on account of the coupling transformer.

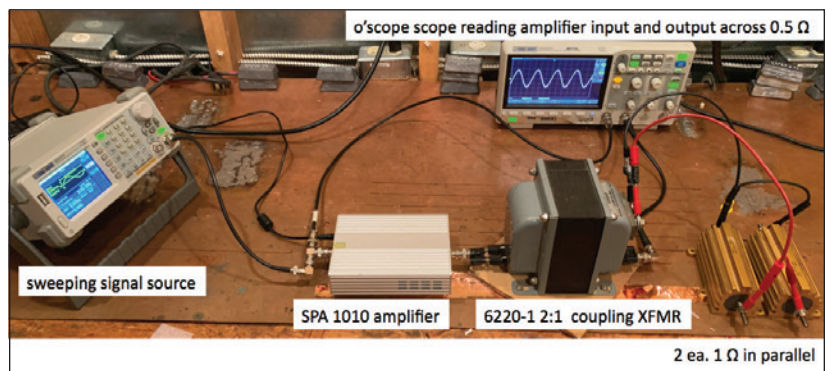


Figure 1: Original measurement set-up calibrating tailored CS101 power limit using SPA1010



Figure 2: Final measurement set-up calibrating tailored CS101 power limit using SPA1010

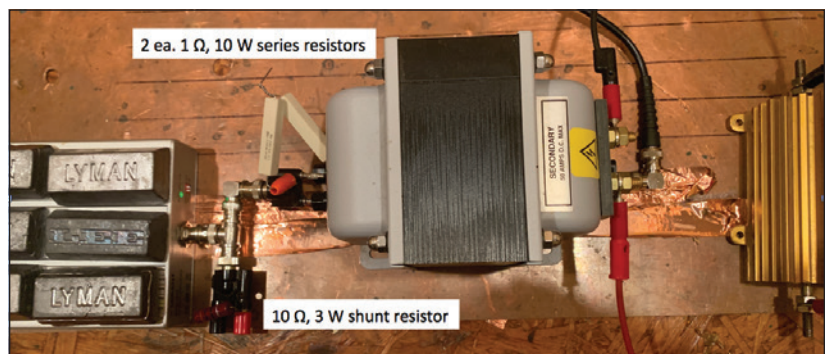
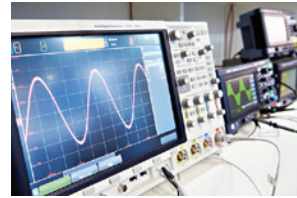


Figure 3: Resistor network between amplifier and coupling transformer

If the test article has insufficient capacitive decoupling in front of its dc/dc converter, it can go unstable, drawing too much switched mode current through the coupling transformer secondary.



LOW POWER AMPLIFIER APPROACH

This approach is limited to the spacecraft-like case where the ripple limit is very low relative to the heritage limits found in References 2-5. Note that Reference 9, which represents a tailoring of MIL-STD-461 for equipment-level EMI testing, already has a low 1 V_{rms} limit.

Figure 1 shows a Siglent SPA1010 10 W dc – 1 MHz amplifier in a CS01/CS101 pre-calibration measurement (see Note 11). This amplifier has 15 k Ω input impedance and very low output impedance (specified to be less than 2 Ω , but in fact measured closer to 10 m Ω). The SPA1010 amplifier is protected against both thermal and input/output overload and initially was quite touchy. When it shuts down to protect itself, that poses a hazard to the test article. Figure 2 shows thermal and overload problems successfully addressed, with the amplifier able to operate at full power (meaning 1 V_{rms} across a 0.5 Ω load, not full amplifier power) for hours at a time. This amounts to 40% of the amplifier's total 10 W rated output.

Comparing Figure 2 to Figure 1, we see lead weights on the amplifier, and 2 Ω (2 each, 1 Ω , 10 W power resistors – series resistors more visible in Figure 3) placed in series between the amplifier output and the primary side input of the Solar Electronics 6220-1 coupling transformer. The lead weights, in addition to pressing the amplifier down against the copper ground plane and heat sinking it that way, also added thermal mass in their own right and were mildly warm to the touch after several hours of full (CS101) power operation (see Note 12). The 2 Ω in series between amplifier and coupling transformer ensures that the amplifier sees a minimum 2 Ω load even when a dead short is placed across the transformer secondary output. The amplifier can operate into 2 Ω all day at the tailored 1 V_{rms} limit level.

Figure 3 shows a fix to ensure that the amplifier shutting down does not insert a millihenry in series between the dc power source and the test article power input. The amplifier's output is shunted by a resistor value high enough to not load the amplifier, but low enough to adequately short out the secondary side inductance when reflected across the transformer windings. A 10 Ω , 3 W resistor was selected for this purpose. Looking back from the secondary side, the impedance seen is 2 Ω in series with 10 Ω shunted by the amplifier output and reduced by the square of

**A BETTER WAY
TO
UL & CSA™**

**Experts who help you from
START TO FINISH**

CE too!



**Design Consulting • Compliance Assistance
Product Testing & Certification Lab**

CertifiGroup.com • 800-422-1651

FREE UL-CSA-CE Compliance Whitepapers

the turns ratio. If the amplifier is out of the picture, there is $12\ \Omega$ across the primary, which reflects across as $3\ \Omega$. That should be low enough to not cause instability in the test article.

Figure 4 shows verification that a load powered through the Solar 6220-1 coupling transformer with amplifier disconnected from the primary sees under $3\ \Omega$ series impedance. The HP 4328A milliohmmeter is ideal for this measurement as its output potential is 1 kHz ac, instead of the more typical dc potential of ohmmeters and millohmmeters. A dc milliohmmeter can only read the resistance of the transformer's secondary winding. The measured value of just under $2.5\ \Omega$ is due to the shunting effect of the secondary winding inductance in parallel with the reflected $3\ \Omega$ off the primary side.

ATTENUATION OF HIGH-POWER AMPLIFIER

Figure 5 shows a typical set-up as per References 1–3 and 6–9 that can dissipate 50/80 W in a $0.5\ \Omega$ load, with the addition of an attenuator between the amplifier and the coupling transformer.

The attenuator was designed for this specific application. Several purposes factored into the design, as follows:

- Attenuate high power output so that an error would not inject significantly more ripple into the test article than desired;

- Provide a well-behaved load for the amplifier regardless of test article impedance so that it does not nuisance trip and cause the test article to see a high impedance reflected across transformer windings; and
- Provide a low and near constant inserted transformer secondary impedance as seen by the test article.

If the limit is such as might be found in References 3–8 but the amplifier's maximum output is much greater than 80 W, the attenuation may be based on that ratio. For this technical tip, the limit is as per reference 9 (1 Vrms) and the amplifier is capable of delivering 100 W into a $2\ \Omega$ load. Based on this and the above considerations, the attenuator was designed to symmetrically match $2\ \Omega$ on input and output and provide a nominal 9 dB attenuation. (Attenuator design details may be found in the Sidebar of this article.).

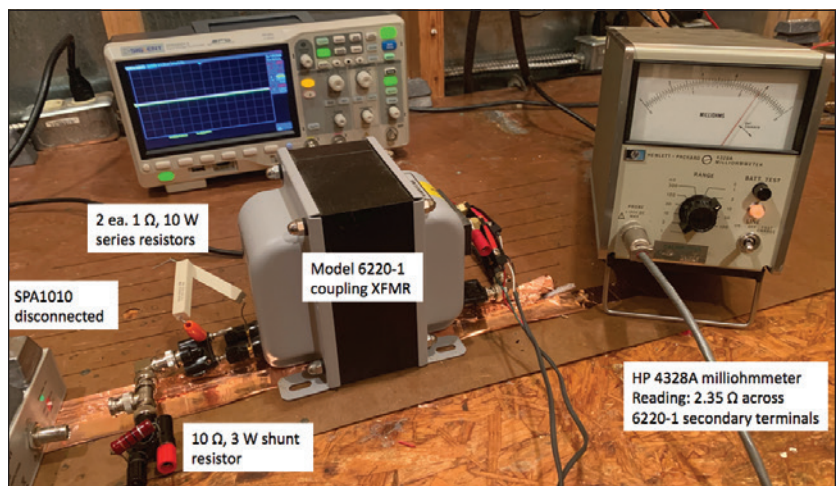


Figure 4: Verification of proper shunting effect by $10\ \Omega$ resistor on SPA1010 output

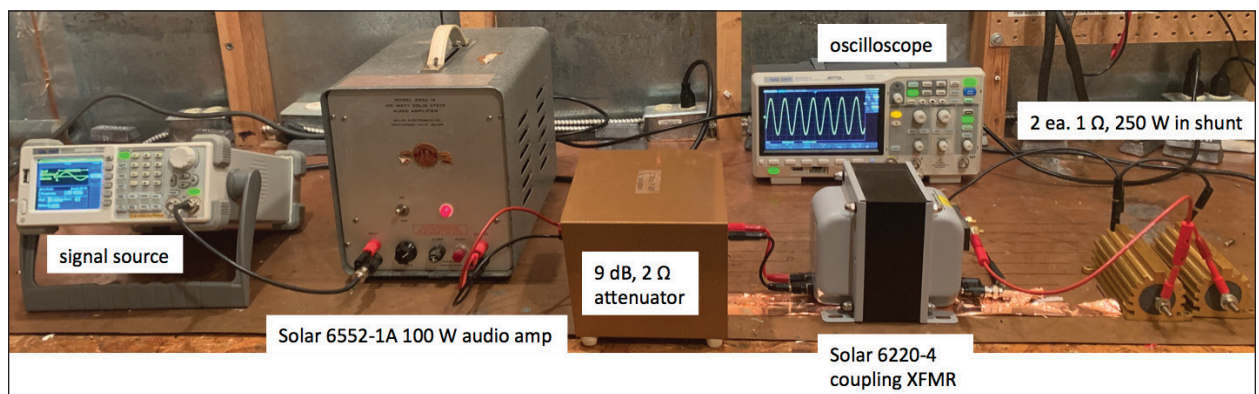


Figure 5: Audio frequency susceptibility set-up using a low resistance attenuator

The proof of the pudding is a repeat of the previous measurements made using the HP 4328A milliohm meter with a 1 kHz ac source signal. The impedance looking into the coupling transformer secondary was measured as a function of the resistance across the input to the attenuator that is connected to the coupling transformer primary. The attenuator input was sequentially open-circuited (as if the amplifier were disconnected, unpowered, or tripped off), connected to a matched 2 Ω (simulating the amplifier’s active output resistance), and then short-circuited.

Table 1 makes it clear that the attenuator is performing the function of making impedance mismatches look much closer to an impedance

match, as does any attenuator properly matched to source and load impedances.

The attenuator only allowed the achievement of a 1 Vrms level across 0.5 Ω through the coupling transformer to just above 100 kHz. At 150 kHz, only 875 mV could be achieved, which is 1.2 dB too low. This is an artifact of the use of this particular amplifier but also the attenuator performance (detailed

Resistance across attenuator input	Measured impedance across secondary	Impedance across secondary if column 1 condition applied directly across XFMR primary (i.e., with attenuator removed)
open	0.66 Ω	6.28 – 10 Ω
match (2 Ω)	0.58 Ω	0.5 Ω
short	0.42 Ω	short

Table 1: Attenuator impedance matching performance (@ 1 kHz)

Fast, Focused, High-Frequency Signals



Intelligent Bi-Polar Power Supply PBZ Series

Perform effective transient tests with the PBZ’s Fast Response and High Frequency. The future of Signal Integrity and Robotics will push for faster speeds and higher power. Kikusui’s combination 4-quadrant supply and signal generator can produce custom waveforms at 100kHz and supplies up to 400W, perfect for testing controllers, motors, inverters, and many other cutting-edge technologies.

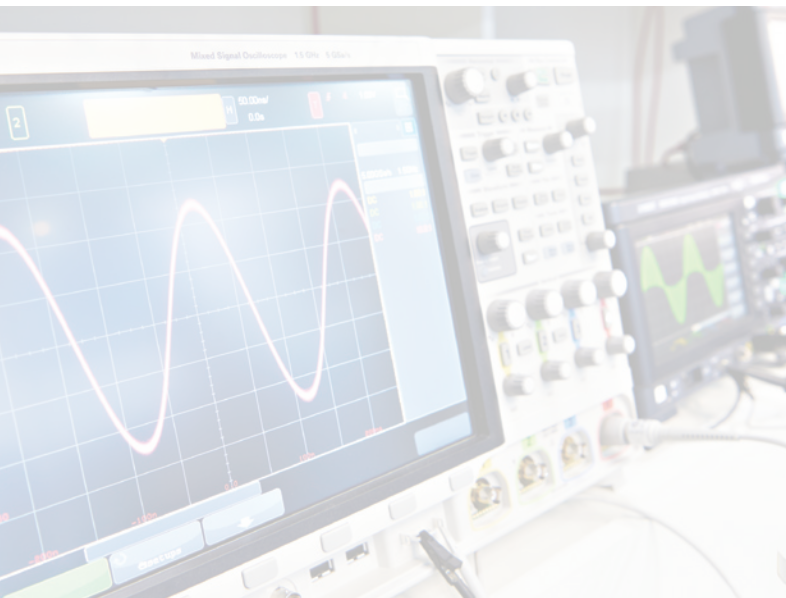


Injection of audio frequency ripple onto power lines requires direct attachment to said power lines and the insertion of considerable series impedance in the form of a transformer secondary.

in the Sidebar). Had the attenuator performance been perfectly flat, the 1 V_{rms} level could have been achieved out to 150 kHz. That being said, this amplifier and the coupling transformer have a high-frequency roll-off such that the maximum unattenuated 150 kHz output across 0.5 Ω through the coupling transformer is about 5 dB down from the 1 kHz 100 W rating. With a higher powered and/or flatter performance amplifier, this condition would not have occurred.

CONCLUSION

Injection of audio frequency ripple onto power lines requires direct attachment to said power lines and the insertion of considerable series impedance in the form of a transformer secondary. Additionally, typically available test equipment can inject much higher levels of ripple than necessary in many applications. Both these conditions can result in damage to the equipment undergoing qualification. If that equipment is of high value, due to cost and/or the schedule impact of damage, then either of the two approaches described herein should be considered to remove those sources of program risk. 📧



REFERENCES/NOTES

1. MIL-STD-462 CS01, *Measurement of Electromagnetic Interference Characteristics*, 31 July 1967.
2. MIL-STD-462D CS101, *Measurement of Electromagnetic Interference Characteristics*, 11 January 1993.
3. MIL-STD-461E-G CS101, *Requirements for the Control of Electromagnetic Interference Characteristics of Subsystems and Equipment*, 1999 – present.
4. MIL-STD-461 basic/A CS01, *Electromagnetic Interference Characteristics Requirements for Equipment*, 1967 – 1980.
5. MIL-STD-461 B/C CS01, *Electromagnetic Emission and Susceptibility Requirements for the Control of Electromagnetic Interference*, 1980 – 1993.
6. RTCA/DO-160 basic-G Section 18, *Environmental Conditions and Test Procedures for Airborne Equipment*, 1975 – present.
7. SAE J1113/2, *Electromagnetic Compatibility Measurement Procedures and Limits for Vehicle Components (Except Aircraft)—Conducted Immunity, 15 Hz to 250 kHz—All Leads*, 1996 – 2010.
8. ISO 11452-10, *Immunity to conducted disturbances in the extended audio frequency range*, 2009 – present.
9. AIAA S-121 8.8, *Electromagnetic Compatibility Requirements for Space Equipment and Systems*, 2009 – present.
10. Javor, Ken, “EMC Archaeology, Uncovering a Lost Audio Frequency Injection Technique,” *In Compliance Magazine*, April 2011.
11. <https://siglentna.com/product/spa1010-10-watt-amplifier>
12. Lead ingots are used for a variety of purposes at the EMCC test facility, and thus were a handy solution. Any technique that removes enough heat is suitable.

Sidebar

The attenuator's purpose is to:

- Attenuate high power output so that a test operator or software error would not inject significantly more ripple into the test article than desired;
- Provide a well-behaved load for the amplifier regardless of test article impedance so that it does not nuisance trip and cause the test article to see a high impedance reflected across transformer windings; and
- Provide a low and near constant inserted transformer secondary impedance as seen by the test article.

Based on these concerns, a 100 W amplifier and a 1 Vrms limit across 0.5 Ω, the attenuator was designed to provide a bidirectional symmetrical match to 2 Ω and attenuate so that it could provide an output of 2.5 V across 2 Ω when a 50 W power amplifier with an output impedance of 2 Ω was driving it (~12 dB). 9 dB was selected to allow 3 dB headroom. Because the amplifier was actually rated for 100 W mid-band (1 kHz), a fuse was incorporated in order to avoid having to choose attenuator component ratings for the higher power.

The only other design consideration is whether a symmetrical “π” or “T” configuration will be chosen. Figure 6 shows π- and T-circuit configurations.

The equations that define the resistor values in Figure 6 in the general case are:

$$\begin{aligned} \text{π-circuit: } R_1 &= R_c (1 - \alpha^2) / 2\alpha, & R_2 &= R_c (1 + \alpha) / (1 - \alpha) \\ \text{T-circuit: } R_1 &= R_c (1 - \alpha) / (1 + \alpha), & R_2 &= R_c \cdot 2\alpha / (1 - \alpha^2) \end{aligned}$$

where

R_c = impedance to match (in our audio case, 2 Ω), &
 α = desired attenuation (in our case, 2.5/7 = 9 dB)

Figure 7 shows a “π” circuit realization with 4 Ω series resistance and 2.5 Ω shunt resistances. Figure 8 shows high-frequency roll-off due to the use of wire-wound high-power resistors. This could have been avoided using non-inductive resistors, at the expense of much greater assembly complexity.

It is important to note that, if the amplifier output impedance is much lower than 2 Ω, then either the attenuator input stage must include the difference, or it must be added externally in series between the amplifier output and attenuator input. Of course, if one is willing to design an attenuator for a specific amplifier, one could match the amplifier's output resistance while retaining the attenuator's output resistance matching to 2 Ω. In that case, the design equations in this sidebar would need to be modified accordingly.

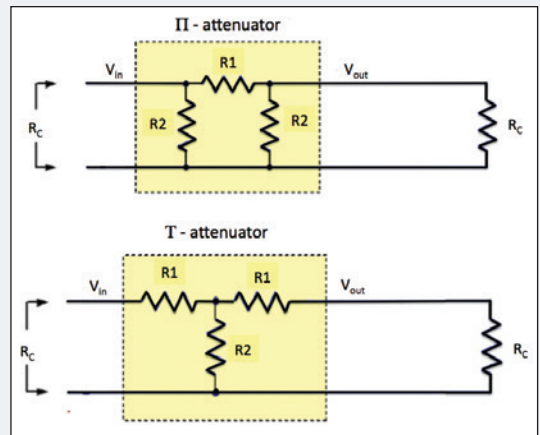


Figure 6: Possible attenuator design topologies

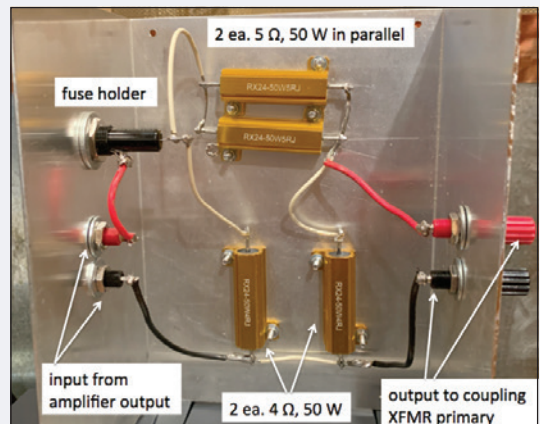


Figure 7: π-configuration attenuator assembly interior construction details

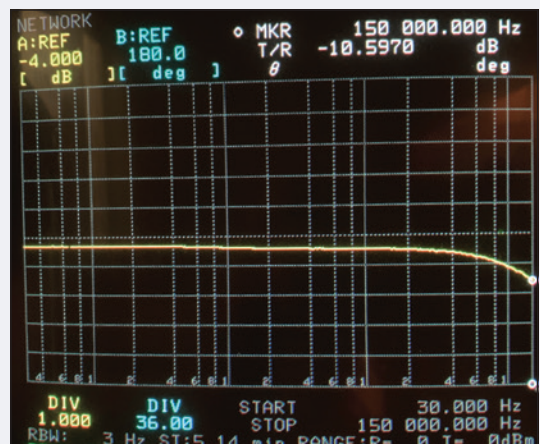


Figure 8: π-attenuator performance (1.3 dB high-frequency roll-off attributed to use of wire-wound power resistors)

SOUTH KOREA KS C 9814-1:2022 STANDARD

Comparison Between KS C 9814-1:2020 and KS C 9814-1:2022



Grace Lin is a Regulatory Compliance Engineer at HYTORC. Prior to HYTORC, she was an EMC Staff Engineer and a TCB Reviewer at Intertek. Lin can be reached at glin@hytorc.com.



By Grace Lin

On May 31, 2022, South Korea's National Radio Research Agency issued Announcement No. 2022-40 stipulating that KS C 9814-1:2022, *Electromagnetic compatibility (EMC) — Requirements for household appliances, electric tools and similar apparatus — Part 1: Emission*, is the latest edition of South Korean emission product standard for household appliances, electric tools, and similar apparatus. KS C 9814-1:2022 is a modified version of CISPR 14-1:2020 Edition 7.0. Significant changes have been made with respect to the previous edition, KS C 9814-1:2020 (CISPR 14-1:2016). This article addresses emission requirements specified in the KS C 9814-1:2022 standard, focusing on the latest changes and deviations from the CISPR 14-1:2020 standard.

SCOPE

The following equipment is explicitly included in the scope of the standard:

- Air conditioning
- Personal care and beauty care appliances
- Electric fence energizers
- Equipment incorporating radio transmit/receive functions
- Equipment under the scope of this document making use of inductive power transfer (IPT)

Equipment making use of IPT technology is introduced in this edition. Many devices, such as electric toothbrushes, use IPT technology to recharge batteries.

Equipment used only in an industrial environment is excluded from the scope of this standard.

NORMATIVE REFERENCES

Referenced standards are now dated, as shown in Table 1.

TERMS, DEFINITIONS, AND ABBREVIATED TERMS

The following terms and definitions are added to the standard:

- System under test
- Ancillary equipment
- Associated equipment
- Representative load
- Representative source
- DC powered equipment

KS C 9814-1:2020	KS C 9814-1:2022	Referenced International Standard
CISPR 16-1-1:2015	KS C 9816-1-1:2020	CISPR 16-1-1:2015
KS C 9816-1-2	KS C 9816-1-2:2021	CISPR 16-1-2:2017
CISPR 16-1-3:2004	KS C 9816-1-3:2021	CISPR 16-1-3:2004/AMD2:2020
KS C 9816-2-1	KS C 9816-2-1:2020	CISPR 16-2-1:2014/AMD1:2017
KS C 9816-2-1	KS C 9816-2-1:2020	CISPR 16-2-2:2010
KS C 9832	KS C 9832:2019	CISPR 32:2015
KS C IEC 60050-161	KS C IEC 60050-161:1990	IEC 60050-161:1990
KS C 9816-1-4	CISPR 16-1-4:2019	CISPR 16-1-4:2019
KS C 9816-2-3	CISPR 16-2-3:2016	CISPR 16-2-3:2016/AMD1:2019
IEC 60335-2-76:2002	(deleted)	-
KS C IEC 61000-4-20	IEC 61000-4-20:2010	IEC 61000-4-20:2010
IEC 61000-4-22	IEC 61000-4-22:2010	IEC 61000-4-22:2010

Table 1: Normative references and equivalent international standards

- Inductive power transfer (IPT)
- IPT source (IPTS)
- Inductive powering equipment
- Inductive cooking appliance
- IPT client (IPTC)
- IPT equipment (IPTE)
- Radio transmitter
- Radio receiver

Terms other than those stipulated in the standard are in accordance with the provisions of the Radio Wave Act, the Enforcement Decree of the Radio Act, the electromagnetic compatibility standards, and the international and national standards related to electromagnetic compatibility.

The following abbreviations are added to the standard:

- AE—associated equipment
- AuxEq—auxiliary equipment
- EMI—electromagnetic interference
- EUT—equipment under test
- FSOATS—free space open area test site
- IPT—inductive power transfer
- IPTS—inductive power transfer source
- IPTC—inductive power transfer client
- IPTE—inductive power transfer equipment
- RBW—resolution bandwidth
- VBW—video bandwidth

LIMITS

Limits are specified based on the following types of equipment: tools, equipment using IPT, electric fence energizers, toys, and others. All toys are in one category, versus five categories in the previous edition.

CONDUCTED DISTURBANCES

Frequency spectrum of conducted emissions measurement is investigated from 9 kHz to 30 MHz. The frequency range of 9 kHz to 150 kHz applies only to equipment with active IPT functions.

Frequency range of 150 kHz to 30 MHz applies to all equipment. The general limits for the mains ports are identical to the CISPR 32:2019 limits for

Class B equipment, except for the average limits in the frequency range of 0.15 to 0.5 MHz (which is 59 dB μ V to 46 dB μ V).

For the discontinuous disturbances on the mains port, with click rate (N) less than 30, the click limit, in the frequency range of 150 kHz to 30 MHz, is calculated by increasing the relevant quasi-peak limit for the continuous disturbances by 44 dB (for $N < 0.2$) or 20 lg (30/N) dB (for $0.2 \leq N < 30$).

RADIATED DISTURBANCES

Frequency spectrum of radiated disturbances measurement is investigated from 30 MHz to 1 GHz, 2 GHz, 5 GHz, or 6 GHz, depending on the highest clock frequency contained in the equipment under test (EUT).

KS C 9814-1 does not specify the fully anechoic room (FAR) testing method for the radiated disturbances measurement. For the frequency range of 30 MHz to 1 GHz, radiated disturbances limits are specified at both 10 m and 3 m measurement distances for both open area test site (OATS) and semi-anechoic chamber (SAC) testing methods. The 3 m measurement distance applies only to the small size equipment.

Radiated disturbances measurement for the frequency range of 1 GHz to 6 GHz is introduced in this edition. Limits are specified at a 3 m measurement distance using the free space open area test site (FSOATS) testing method. An FSOATS is a SAC or an OATS with RF absorbers on the reference ground plane (GRP).

Radiated disturbances limits are identical to the CISPR 32:2019 limits for Class B equipment.

TEST CONDITIONS

Test conditions for the following equipment are revised or added:

- Clothes irons
- Personal care appliances
- Battery chargers
- Robotic equipment
- Equipment making use of IPT
- Remote controls and timers

FIGURES

Table 2 shows the changes made to the figures.

Figure Number		Description
CISPR 14-1:2020 KS C 9814-1:2022	CISPR 14-1:2016 KS C 9814-1:2020	
1	-	IPT terms
-	1	Possible issue due to a high standard deviation when using method 7.3.3
2	-	Examples of test configuration
3	2	Examples of discontinuous disturbances whose duration and separation meet the definition of clicks (see 3.3.3)
4	3	Examples of discontinuous disturbances whose duration and separation meet the definition of clicks (see 3.3.3)
5	4	Flow chart for emission measurements of mains operated equipment in the frequency range from 30 MHz to 1,000 MHz
6	5	Flow chart for emission testing of battery-operated equipment in the frequency range from 30 MHz to 1,000 MHz
7	-	Flow chart for emission measurements in the frequency range from 1 GHz to 6 GHz
-	6	Flow diagram for measurements of discontinuous disturbance
8	-	Flow diagram for the evaluation of discontinuous disturbance, based on measuring the clicks
9	-	Flow diagram for the evaluation of discontinuous disturbance, based on counting the switching operations
10	7	Artificial hand – RC element
11	8	Application of the artificial hand – Portable electric drill
12	9	Application of the artificial hand – Portable electric saw
13	10	Cable bundling
14	11	Voltage probe measurement for mains-powered EUT
15	12	Radiated emission – Location of the EUT on the turntable and measuring distance
16	13	Radiated emission – Example of test set-up for table-top EUT
17	14	Radiated emission – Example of test set-up for table-top EUT
18	15	Radiated emission – Example of test set-up for table-top EUT (top view)
19	16	Radiated emission – Example of test set-up for floor-standing EUT
20	17	Radiated emission – Example of the test set-up for an EUT made of multiple table-top parts
21	18	Radiated emission – Example of the test set-up for an EUT in SAC or OATS, made of a combination of table-top and floor standing parts
22	19	Radiated emission – Height of the EUT in the FAR
23	-	Example of test setup for disturbance voltage measurements on table-top EUT (horizontal RGP)
24	-	Example of alternative test setup (vertical RGP) for measurements on table-top EUT (disturbance voltage on mains port and disturbance current on auxiliary port)
25	-	Example of disturbance voltage measurement arrangement for floor standing EUT(s)

Table 2: Figure number comparison

TABLES

Table 3 shows the changes made to the tables.

CONCLUSION

Keeping up with standard changes shortens product design cycle, speeds up product launch, and leads to success of business. This article lists key changes made to the standard to save much of research time. 

REFERENCES

- KS C 9814-1:2022, *Electromagnetic compatibility (EMC) - Requirements for household appliances, electric tools, and similar apparatus - Part 1: Emission* (MOD CISPR 14-1:2020).
<https://e-ks.kr/streamdocs/view/sd;streamdocsId=72059240219206861>

Table Number		Description
CISPR 14-1:2020 KS C 9814-1:2022	CISPR 14-1:2016 KS C 9814-1:2020	
1	1	Application of limits
2	-	Disturbance voltage limits for the AC mains port of equipment with active IPT functions
-	2	Disturbance voltage limits for induction cooking appliances
3	3	Magnetic field strength limits
4	4	Limit for the magnetic field-induced current
5	5	General limits
6	-	Limits for the mains port of motor-operated tools
-	6	Limits for mains port of tools
7	7	Disturbance power limits – 30 MHz to 300 MHz
8	8	Reduction application to Table 7 limits
9	9	Radiated disturbance limits and testing methods – 30 MHz to 1,000 MHz
10	-	Required highest frequency for radiated electric field strength measurements
11	-	Radiated electric field disturbance limits and test methods – 1 GHz to 6 GHz
A.1	-	Types of EUT, operating modes and test setup
B.1	B.1	Application of factor f for the determination of the click rate of special equipment
C.1	-	Discontinuous disturbances recorded during the first run at 500 kHz
C.2	-	Discontinuous disturbances recorded during the second run at 500 kHz
C.3	-	Discontinuous disturbances recorded during the first run at 1.4 MHz
C.4	-	Discontinuous disturbances recorded during the second run at 1.4 MHz
C.5	-	Examples of minimum observation time
D.1	11	Values of the coefficient K_E as a function the sample size
D.2	10	General margin to the limit for statistical evaluation
D.3	12	Factor k for the application of the non-central t-distribution
D.4	13	Application of the binomial distribution

Table 3: Table number comparison

- KS C 9814-1:2020, *Electromagnetic compatibility (EMC) – Requirements for household appliances, electric tools and similar apparatus – Part 1: Emission* (MOD CISPR 14-1:2016).
<https://e-ks.kr/streamdocs/view/sd;streamdocsId=72059202823552187>
- KS C 9832:2019, *Electromagnetic compatibility of multimedia equipment — Emission requirements* (MOD CISPR 32:2015).
<https://e-ks.kr/streamdocs/view/sd;streamdocsId=72059198987155269>
- CISPR 14-1 2020-09 Edition 7.0, *Electromagnetic compatibility – Requirements for household appliances, electric tools, and similar apparatus – Part 1: Emission.*
- CISPR 14-1 2016-08 Edition 6.0, *Electromagnetic compatibility – Requirements for household appliances, electric tools, and similar apparatus – Part 1: Emission.*



www.raymondemc.com

QUIET MATTERS.

Whatever your project needs to shield, we can create it.

We design, engineer, build, and install quality turnkey, shielded enclosures and anechoic solutions to meet your project's requirements and specifications.

EMC Chambers | Deployable Chambers | Anechoic Chambers | Shielded Enclosures | Shielded Doors | Shielded Cabinets | Shielded Bags and Tents | Chamber Accessories | Consulting Services | Installations Services | Chamber Relocation Services | Maintenance/Repairs/Upgrades

sales@raymondemc.com

1-800-EMC-1495

HEALTH MONITORING AND PREDICTION OF CELLS IN A BATTERY MODULE OR PACK UNDER OPERATING CONDITION

A Nondestructive and Cost-Effective Approach



Benjamin Chen is an independent engineering consultant and can be reached at benjamin.s.chen.tw@outlook.com.



By Benjamin Chen

Editor's Note: The paper on which this article is based was originally presented at the 2021 IEEE International Symposium on Product Compliance Engineering – Asia (ISPCE-ASIA), held in Taipei, Taiwan in November/December 2021. It is reprinted here with the gracious permission of the IEEE. Copyright 2021, IEEE.

INTRODUCTION

Following the growth in the fire incidents of electric vehicles (EVs) and energy storage systems (ESSs) after years of operation, the health monitoring system of EVs and ESSs are still a concerned topic. While it is relatively easy to measure health condition of a cell under static condition, the health condition measurement over cell packed into a system and under operating condition is rather difficult or time consuming with static measurement methodologies.

However, the deterioration of one cell in a series block will reduce the performance of the whole block, and the deterioration will lead to economic concerns like life span depreciation or mileage cost, so it is very important to develop a health monitoring system without the interruption of actual operation and disassembly of battery pack into modules and cells.

DYNAMIC BEHAVIOR DESCRIPTION OF CELL PERFORMANCE IN LAB ENVIRONMENT

Considering the importance of cell condition under heavy duty and long-life demand in EV application, IEC/ISO has published performance standard IEC 62660-1:2018 for the cell and ISO 12405-4:2018 for the pack. Both standards emphasize the performance of cell under dynamic charge and discharge behaviors, not only in battery electric vehicles (BEVs) but also hybrid electric vehicles (HEVs).

Those dynamic profiles have taken conditions into consideration, such as:

1. Regenerative braking;
2. Road driving, accelerating and deceleration, and at different period; and
3. Mode switching from discharge rich at high state of charge (SOC) to charge rich at low SOC.

Testing profile simulating real life operation are created accordingly as can be shown in Figure 1 and Figure 2 from IEC and ISO standards.

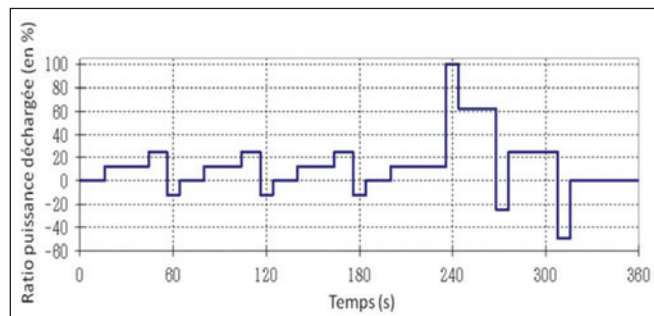


Figure 1: The dynamic discharge profile A for BEV cycle test in IEC 62660-1 [1]

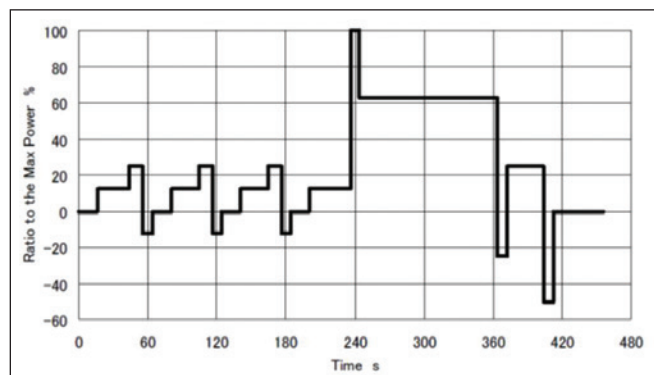


Figure 2: The dynamic discharge profile B for BEV cycle test in IEC 62660-1 [2]

BATTERY HEALTH CONDITION BY ELECTRO-IMPEDANCE SPECTROSCOPY

As most research study referenced, EIS was considered as a comprehensive description of battery structures as shown in Figure 3. Typical EIS was conducted by measurement of applying an AC potential to an electrochemical cell and then measuring the current through the cell under various frequency, usually from frequencies as low as 1mHz to as high as 1MHz.

The responsive frequency can be considered as a description of cell electrochemical structure, as there are many layers of materials between electrodes, and the external potential is like a tuning fork set with in different vibration frequencies. Each layer material has different characteristic natural frequency and will be in resonance when the voltage frequency is the same. The amplitude of the characteristic frequency peak can be analogous to the thickness or the mass of the material. When the material is thicker, the response is stronger.

However, a single spectrum at one time for a cell does not constitute any meaning, but when comparing spectrums across cell when the layer thicknesses changed under different operating conditions, the response changes between extremes condition, e.g., SOC 0% to SOC 100%, will help users to estimate the condition under the measurement to the original unused condition.

PERFORMANCE MEASUREMENT UNDER OPERATING CONDITIONS

Establishment of Cell Data by Leveraging BMS

As a voltage of single lithium-ion battery or cell is only 3 volts, creating an output at 12 volts, 48 volts, 96 volts or even above for large powers more than 5 KWs without DC/DC voltage transformation technologies will need to combine cells into series blocks. However, as electrochemical cells do have internal resistance differences, and the voltage difference is greater in the end of blocks. To avoid overvoltage of cells in the block, based on the module safety standard requirement like IEC 62133, UL 2594, or UL 2580, each cell in the same series is required to integrate overvoltage prevention mechanisms or monitoring systems, as shown in Figure 4.

Accordingly, most of manufacturers install voltage sensor onto each cell or cell block of the same series and collect the voltage data into the BMS system within the module or pack or send out to downstream storage or analyzing devices like programmable logic controllers (PLC), industrial personal computer (IPC), or cloud computing or storage services by wired communication interface like controller area network (CAN) bus, Modbus, Ethernet, or wireless like WIFI, Bluetooth, or 4G.

Through the data retrieved from BMS system plotted with time, the slope of charge/discharge response or the shape of voltage recovery, can then be applied to the cell EIS database for further analysis.

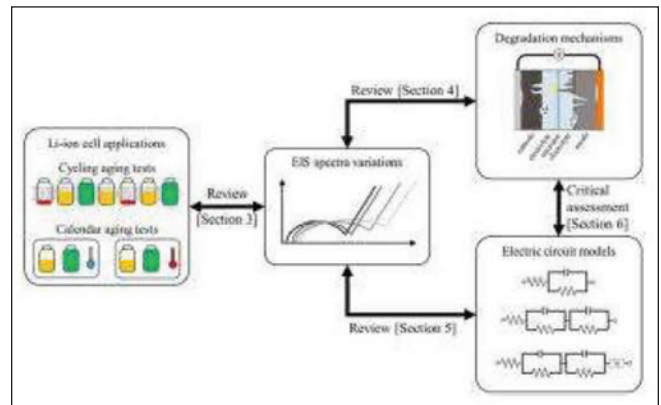


Figure 3: Concepts of EIS and its relationships to the electrochemical structure of a cell [3]

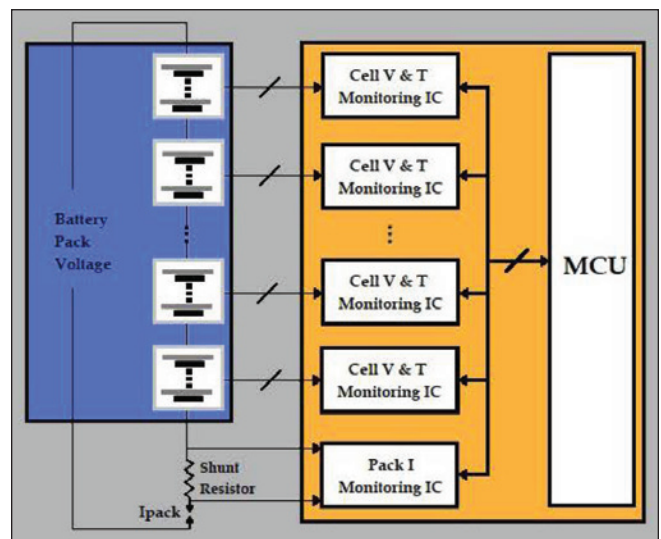


Figure 4: Typical cell monitoring wiring schemes to BMS in a battery module [4]

Though not perfectly controlled like laboratory environment with standardized power supply and electrical loads, the voltage sensor, current sensor, and temperature sensor with power controlling system (PCS), battery charger/discharger, and the motor or actually load, and BMS do constitute a similar testing system also providing continuous and meaningful data.

Establishment State of Health Profiles by EIS-Like Database

As can be imagined, EIS is typically conducted on single cell at laboratory conditions, and a complete scan from 1 mHz to 1MHz will take several hours to complete. It is not economically feasible to conduct EIS over each cell in a pack, and impossible without disassembly and also under operation.

However, each charge and discharge under different potential and time in real operation is like a pulse of EIS scan, and then we can reconstruct an EIS like spectrum after voltage normalization though may not be continuous in frequencies.

By accumulation of spectrum across different cells and time against real behavior or performance, user or manufacturer can define a database of cell health condition, similar to study as shown in Figure 5.

Data Processing and Report Preparation

When the database of SOH for the interested cell or electrochemical structure was established, the voltage, current, SOC, and time information can be retrieved by BMS then send to edge devices like computers or mobile phones, or directly to cloud for comparison. An overall distribution of SOH for cells in the pack can be drawn as visualized in 3D or 2D objects, similarly to the diagrams shown in Figure 6.

CONCLUSION

The SOC information of a cell is important as the baseline information, but EIS or dynamic behavior information is more comprehensive and important for the description of SOH. Through the data processing retrieved from BMS under real time operation and comparing with the database established with existing SOH profile, the SOH distribution for the cells in the pack can be described and demonstrated without disassemble the battery pack back to cells under dynamic and operating conditions.

The similar approach can be applied to ESS as well as long as BMS data are available by communication interfaces and regardless of battery chemistries. 

REFERENCES

1. <https://ec.europa.eu/research/participants/documents/downloadPublic?documentIds=080166e5a1622586&appId=PPGMS>
2. Energies 2012, 5, 138-156; doi:10.3390/en5010138, Standardization Work for BEV and HEV Applications: Critical Appraisal of Recent Traction Battery Documents
3. <https://en.x-mol.com/paper/article/1399478987489001472>
4. <https://circuitdigest.com/article/battery-management-system-bms-for-electric-vehicles>
5. <https://www.battpedia.com>
6. <https://battpedia.com/battery/battpedia-battery-aging-simulator>



Figure 5: The database of SOH profiles for various brands and electrochemical structures [5]

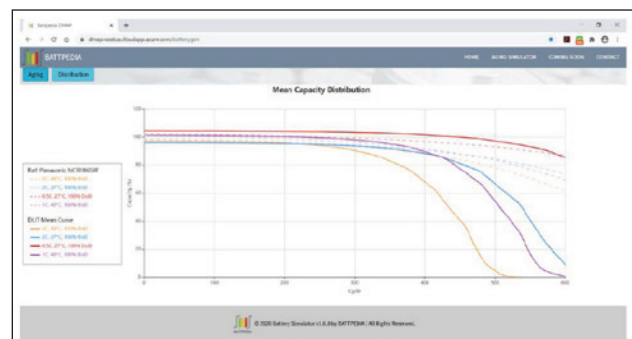


Figure 6: The prediction of cell SOH under different operating conditions [6]

SHUNT INDUCTIVE DISCONTINUITY ALONG THE TRANSMISSION LINE AND TRANSMISSION LINES IN PARALLEL

By Bogdan Adamczyk

This article discusses the impact of a shunt inductive discontinuity along the line as well as the effect of feeding two transmission lines in parallel. The analytical results are verified through the HyperLynx simulations and laboratory measurements.

1.1 REFLECTIONS AT THE SHUNT INDUCTIVE DISCONTINUITY - ANALYSIS

Consider the circuit shown in Figure 1.1, where the transmission line of length l has a shunt inductive discontinuity in the middle of the line at a location $z = d$.

Note that the transmission line is matched at the source and at the load; it is also assumed that the initial current through the inductor is zero, $i_L(0^-) = 0$.

When the switch closes at $t = 0$, a wave originates at $z = 0$, [1], with

$$v_i = \frac{V_G}{2} \tag{1.1a}$$

$$i_i = \frac{V_G}{2Z_C} \tag{1.1b}$$

and travels towards the discontinuity. When this wave arrives at the discontinuity (at the time $t = T$), the reflected waves, v_r and i_r are created. The transmission line immediately to the right of the discontinuity looks to the circuit on the left of the discontinuity like a shunt resistance equal to the characteristic impedance of the right line [2]. Figure 1.2 illustrates this.

The reflected current wave is related to the reflected voltage wave by

$$i_r(t) = -\frac{v_r(t)}{Z_C} \tag{1.1c}$$

KVL and KCL at the discontinuity produce

$$v_i + v_r(t) = v_L(t) \tag{1.2a}$$

$$i_i + i_r(t) = i_L(t) + i_R(t) \tag{1.2b}$$

Dr. Bogdan Adamczyk is professor and director of the EMC Center at Grand Valley State University (<http://www.gvsu.edu/emccenter>) where he regularly teaches EMC certificate courses for industry. He is an iNARTE certified EMC Master Design Engineer. Prof. Adamczyk is the author of the textbook “Foundations of Electromagnetic Compatibility with Practical Applications” (Wiley, 2017) and the upcoming textbook “Principles of Electromagnetic Compatibility with Laboratory Exercises” (Wiley 2022). He can be reached at adamczyk@gvsu.edu.



Our initial goal is to determine the reflected voltage $v_r(t)$ at the location $z = d$, i.e., $v_r(d, t)$. The ultimate goal is to determine the total voltage at the discontinuity, $v_L(d, t)$.

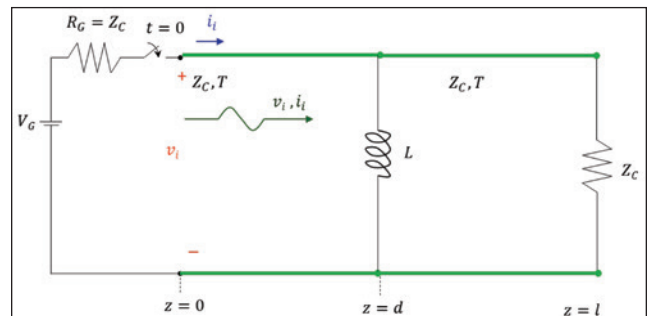


Figure 1.1: Shunt inductive discontinuity along a transmission line

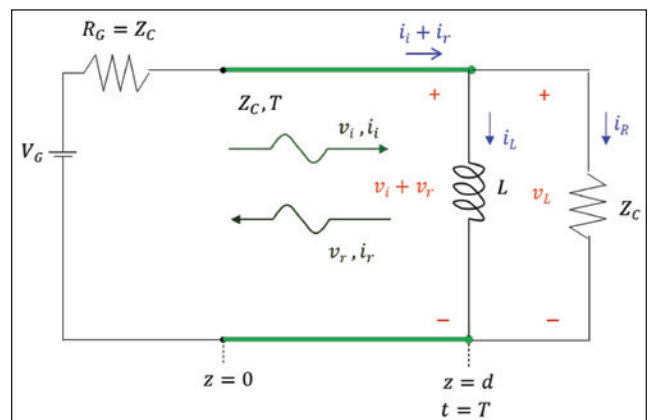


Figure 1.2: Incident and reflected waves at the inductive discontinuity

The current $i_R(t)$ can be expressed as

$$i_R(t) = \frac{v_i + v_r(t)}{Z_C} \quad (1.3)$$

From Eq. (1.2b), we obtain the inductor current as

$$i_L(t) = i_i + i_r(t) - i_R(t) \quad (1.4)$$

Utilizing Equations (1.1b), (1.1c), and (1.3) in (1.4) we get

$$i_L(t) = \frac{V_G}{2Z_C} - \frac{v_r(t)}{Z_C} - \frac{V_G}{2Z_C} - \frac{v_r(t)}{Z_C} = -2 \frac{v_r(t)}{Z_C} \quad (1.5)$$

The differential v - i relationship for the inductor is

$$v_L(t) = L \frac{di_L(t)}{dt} \quad (1.6)$$

Using Equations (1.1a), (1.2a), and (1.5) in Eq. (1.6) we obtain

$$\frac{V_G}{2} + v_r(t) = L \frac{d}{dt} \left[-2 \frac{v_r(t)}{Z_C} \right] \quad (1.7)$$

or

$$\frac{dv_r(t)}{dt} + \frac{v_r(t)}{2L/Z_C} = \frac{V_G Z_C}{4L} \quad (1.8)$$

This differential equation needs to be solved for $v_r(t)$, for $t > T$, subject to the initial condition $v_r(t = T)$.

Let's determine this initial condition.

Initially, the current through an inductor $i_L(T)$ is zero. Thus, the inductor acts as an open circuit, and the incident wave sees the discontinuity as a matched load. Therefore, there is no reflection and

$$v_r(T) = 0 \quad (1.9)$$

Eq. (1.8) can be written as

$$\frac{dv_r}{dt} + \frac{v_r}{\tau} = K \quad (1.10)$$

where

$$\tau = \frac{2L}{Z_C}, \quad K = -\frac{V_G Z_C}{4L} \quad (1.11)$$

The solution of Eq. (1.10) was derived in [2] as

$$v_r(t) = K\tau + [v_r(T) - K\tau]e^{-\frac{1}{\tau}(t-T)} \quad (1.12)$$

Utilizing Equations (1.9) and (1.11) in Eq. (1.12), we obtain

$$v_r(d, t) = -\frac{V_G}{2} + \frac{V_G}{2} e^{-\frac{(t-T)}{2L/Z_C}}, \quad t \geq T \quad (1.13)$$

The total voltage across the discontinuity is

$$v_L(d, t) = v_i + v_r(d, t) = \frac{V_G}{2} + v_r(d, t) \quad (1.14a)$$

or

$$v_L(d, t) = \frac{V_G}{2} e^{-\frac{(t-T)}{2L/Z_C}}, \quad t \geq T \quad (1.14b)$$

Equation (1.14b) predicts that at $t = T$, the voltage at the load rises from zero to $V_G/2$ and then decays exponentially to z . Let's verify these observations through simulations and measurements.

1.2 REFLECTIONS AT THE INDUCTIVE DISCONTINUITY - SIMULATION

Figure 1.3 shows the HyperLynx schematic of the transmission line with an inductive discontinuity.

The simulation results are shown in Figure 1.4.

Note that the simulation results verify the analytical results.

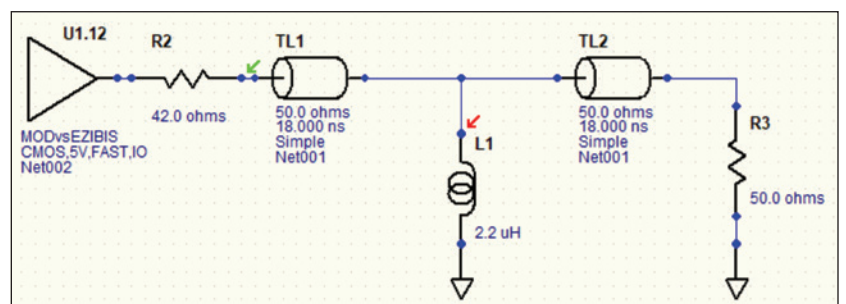


Figure 1.3: Inductive discontinuity - HyperLynx schematic

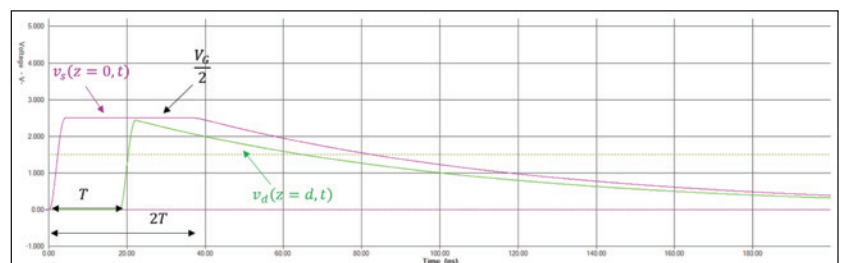


Figure 1.4: Inductive discontinuity - Voltages at the source ($z = 0$) and the load ($z = d$)

1.3 REFLECTIONS AT THE INDUCTIVE DISCONTINUITY - MEASUREMENTS

The measurement setup is shown in Figure 1.5.

The measurement results are shown in Figure 1.6.

Note that the measurement results verify the simulation and analytical results.

2.1 FEEDING TRANSMISSION LINES IN PARALLEL - ANALYSIS

Consider the circuit shown in Figure 2.1, where the transmission line of length d is connected to the two other transmission lines.

Note that load resistors are matched to the transmission lines, and all transmission lines have the same characteristic impedances. This makes the

simulations and measurements easier to follow since there are no reflections at the loads.

When the switch closes at $t = 0$, a wave originates at $z = 0$ and travels towards the discontinuity. The transmission lines immediately to the right of the discontinuity look to the circuit on the left of the discontinuity like two resistances in parallel. Their values are equal to the corresponding values of their characteristic impedances. When the incident wave arrives at the discontinuity (at the time $t = T$), the reflected wave, v_r and i_r , is created, and we have a situation depicted in Figure 2.2.

This part of the circuit is identical to the one discussed in [3] where the transmission line had a shunt resistive discontinuity. Thus, the total voltage across at the discontinuity is

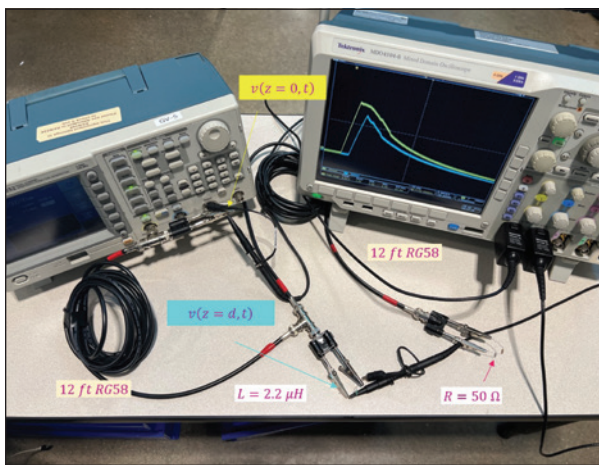


Figure 1.5: Inductive discontinuity – Measurement setup

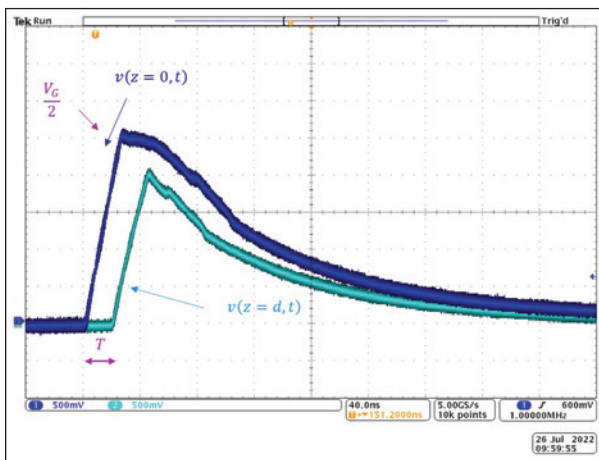


Figure 1.6: Inductive discontinuity – Measurement results

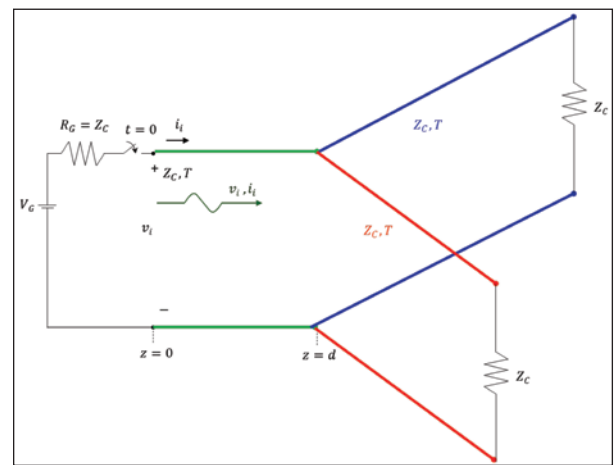


Figure 2.1: Transmission lines in parallel

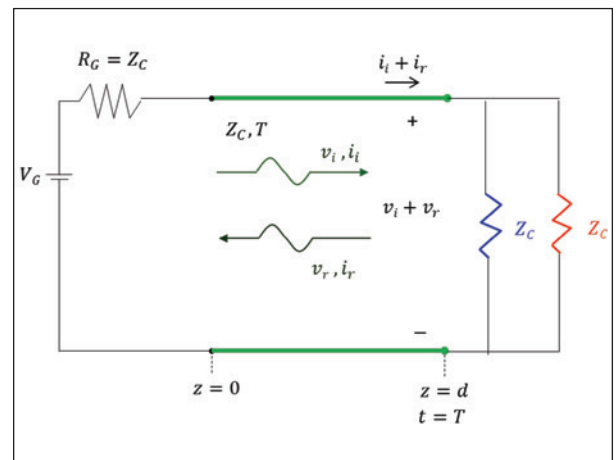


Figure 2.2: Incident and reflected waves at the discontinuity

$$v(z = d, t) = \frac{V_G}{3}, \quad t > T \tag{2.1}$$

and the total voltage at the source (after $t = 2T$) is

$$v_s = v_i + v_r = \frac{V_G}{3}, \quad t > 2T \tag{2.2}$$

- Adamczyk, B., *Foundations of Electromagnetic Compatibility with Practical Applications*, Wiley, 2017.
- Adamczyk, B., "Transmission Line Reflections at a Shunt Resistive and Reactive Discontinuity Along the Line," *In Compliance Magazine*, October 2022.

2.2 FEEDING TRANSMISSION LINES IN PARALLEL - SIMULATIONS

Figure 2.3 shows the HyperLynx schematic of the transmission line in parallel.

The simulation results are shown in Figure 2.4.

2.3 FEEDING TRANSMISSION LINES IN PARALLEL - MEASUREMENTS

The measurement setup is shown in Figure 2.5.

The measurement results are shown in Figure 2.6.

Note that the measurement results verify the simulation and analytical results. 

REFERENCES

- Adamczyk, B., "Transmission Line Reflections at a Resistive Load," *In Compliance Magazine*, January 2017.

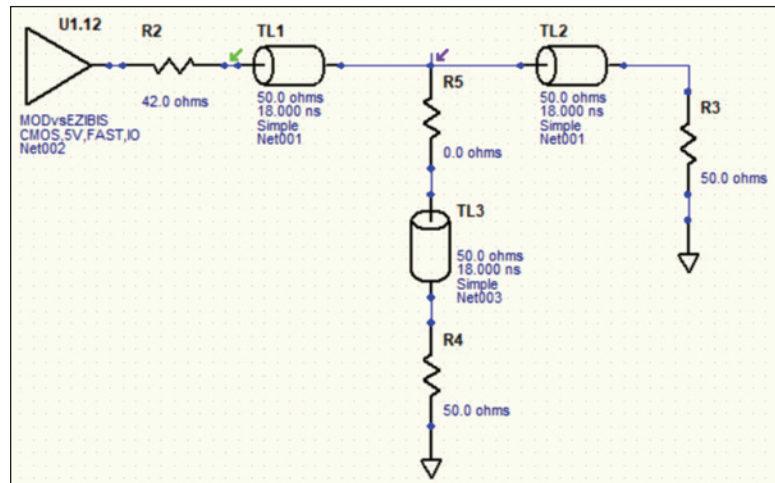


Figure 2.3: Transmission lines in parallel - HyperLynx schematic

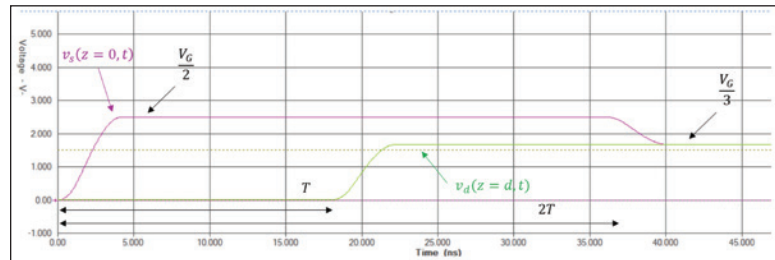


Figure 2.4: Transmission lines in parallel - voltages at the source ($z = 0$) and the discontinuity ($z = d$)

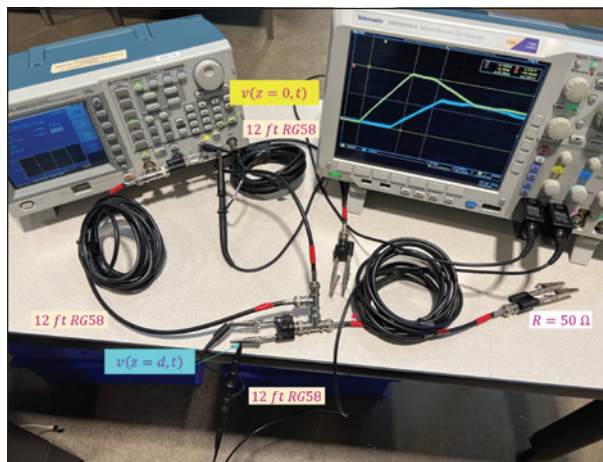


Figure 2.5: Transmission lines in parallel – Measurement setup

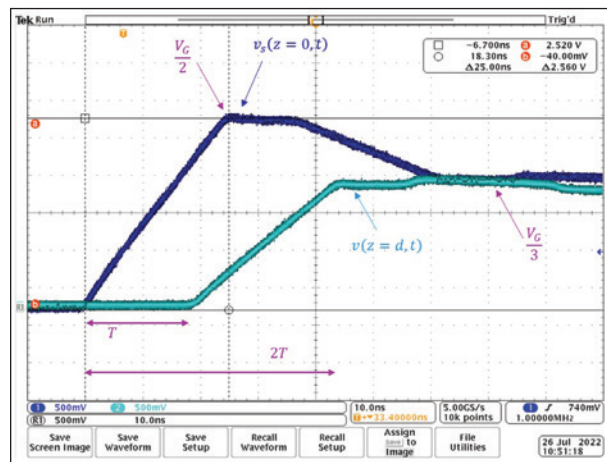


Figure 2.6: Transmission lines in parallel – Measurement results

COMMERCIAL VERSUS AUTOMOTIVE ESD INTEGRATED CIRCUIT QUALIFICATION PART 2

By Robert Ashton for EOS/ESD Association, Inc.

INTRODUCTION

This is Part 2 of an article describing the difference between the electrostatic discharge (ESD) qualification requirements for automotive and standard commercial integrated circuits. Part 1 of the article, in last month's issue of *In Compliance*, described why it is reasonable for automotive products to have higher qualification requirements, describes the documents that specify the requirements for commercial and automotive integrated circuit qualification and the high-level differences between ESD qualification for automotive and commercial integrated circuits. Part 2 describes the additional requirements for automotive ESD testing for human body model (HBM) and charged device model (CDM).

(This article had its origin in a series of blog posts on ESD testing available at <http://www.srftechnologies.com/ESD-RESOURCES.html>.)

Note: This article will summarize the differences between automotive and commercial ESD testing of integrated circuits but should not be used as a substitute for a thorough reading of the actual test methods.

HBM

HBM testing is specified by ANSI/JEDEC/ESD JS-001 [1] with additional requirements specified in AEC-Q100-002 REV-E [2]. This section summarizes the additional requirements for automotive HBM testing.

Waveform Requirements (Q100-002 Section 1.1)

The tester must meet the waveform requirements at all test levels. (Legacy wording in JS-001 could be interpreted that the tester didn't need to meet all waveform requirement at all voltages, but this was never the intention.)

Robert Ashton is the Chief Scientist at Minotaur Labs, a provider of ESD and latch-up testing located in Mesa, Arizona. Robert is an active member of ESDA working groups for device testing standards and the JEDEC latch-up working group. He has been a regular member of the EOS/ESD Symposium technical program committee. He is currently serving as co-chair of the human metal model (HMM) working group.



Founded in 1982, EOS/ESD Association, Inc. is a not for profit, professional organization, dedicated to education and furthering the technology Electrostatic Discharge (ESD) control and prevention. EOS/ESD Association, Inc. sponsors educational programs, develops ESD control and measurement standards, holds international technical symposiums, workshops, tutorials, and foster the exchange of technical information among its members and others.



Test Fixture Board Qualification (Q100-002 Section 2)

Requires the test fixture board to meet waveform requirements at all test voltages, not limited voltages. Also specifies requalification if the board is repaired.

Device Stressing (Q100-002 Section 3)

Requires that device stressing be done at 500 V, 1000 V and 2000 V. Levels may not be skipped. JS-001 allows testing at a single level to establish the immunity level. Q100-002 also specifies that if the device fails 500 V, it requires testing at 250 V, and if that fails testing at 125 V if the tester can meet the waveforms.

Devices with 6 pins or less (Q100-002 Section 4.1)

Devices with 6 pins or less must be tested with all pin pair combinations. (One pin on Terminal A and one pin on Terminal B.) JS-001 requires that discrete devices be tested with all pin combinations and allows devices with 10 or less pins to be tested with all pin pair combinations.

One of the most significant differences between JS-002 and Q100-011 is the number of zaps to each pin per voltage and polarity. Q100-011 requires 3 stresses on each pin for each voltage and polarity, while JS-002 requires “at least 1 discharge” per voltage and polarity.

Pin Combination Table (Q100-002 Section 4.2)

JS-001 includes two options for pin combinations. Table 2B is the traditional pin combinations from the original version of JS-001 and is the same set of pin combinations as in the now obsolete HBM standards from JEDEC and ESDA. Table 2A is a new table which reduces the number of stresses on an integrated circuit but requires more understanding of the device under test. The purpose of Table 2A is to reduce test time and, possibly more important, to reduce failures due to wear out. Q100-002 requires all testing to start using Table 2B. Q100-002 does give three situations in which Table 2A may be used.

- A low parasitic tester is being used
- If a failure using Table 2B is deemed to be a false failure
- If the use of Table 2B leads to failures from wear out due to cumulative stress

Low Parasitic Tester (Q100-002 Section 4.3)

Q100-002 has special instructions if using a low parasitic tester such as a two-pin tester.

- Connectivity must be verified for each stress
- Non-supply to non-supply stress may be done using Table 2A
- All adjacent non-supply pins must be stressed versus each other
- The options in JS-001 Section 6.6 for low parasitic HBM testers may be used.

Reporting (Q100-002 Section 5.0)

Q100-002 has a section on reporting, which is lacking in JS-001. In addition to reporting the basic test results the reporting section requires information on the type of tester used, details on the samples and test details such as pin groupings, stress voltage levels, any partitioning of stress over multiple devices,

stress pin combinations, and any exceptions for the tests performed.

CDM

CDM testing is specified by ANSI/JEDEC/ESD JS-002 [3] with additional requirements specified in AEC-Q100-011 Rev-D [4]. This section summarizes the additional requirements for automotive CDM testing.

Stress Levels Tested (Q100-011 Sections 2.3 and 2.5)

250 V is a required test level, and if higher withstand levels are to be reported testing must be done in 250 V increments up to the highest passing level. It is not permissible to skip stress levels. If a device fails at 250 V testing is to be done at 125 V and if failure occurs at that level lower levels such as 100 V and 50 V are to be used. JS-002 allows testing at a single voltage and if all requirements are met that level can be used as the devices CDM withstand level.

Discharge Requirements (Q100-011 Section 2.5)

One of the most significant differences between JS-002 and Q100-011 is the number of zaps to each pin per voltage and polarity. Q100-011 requires 3 stresses on each pin for each voltage and polarity, while JS-002 requires “at least 1 discharge” per voltage and polarity. The wording of “at least 1 discharge” was added to JS-002 so that a single set of testing could cover both JS-002 and AEC Q100-11 testing.

Corner Pin Classification (Q100-11 Sections 1.3.1 and 2.6)

A unique feature of the AEC CDM is the corner pin requirement. As discussed in Section 2 the standard qualification level for CDM is 500 V, with corner pins at 750 V. Section 1.3.1 of AEC Q100-11 describes the definition of a corner pin, while Section 2.6 describes

The ESD requirements for commercial versus automotive qualification are very similar. Both require HBM and CDM testing based on the same two test standards, JS-001 for HBM and JS-002 for CDM.

two methods to determine the 750 V corner pin classification.

Small Package Considerations (Q100-11 Section 2.7)

This section of Q100-11 discusses the difficulties of CDM testing of small package, and notes that in some cases the testing may need to be skipped, but this must be noted and done in agreement with the user. AEC-Q100-011 Rev-D was published before JS-002-2018 added provisions to eliminate further CDM testing of small devices within a technology family with a known CDM history of robustness.

Wafer or Bare Die Considerations (Q100-11 Section 2.8)

This section discusses CDM testing of products shipped at wafer level or as bare die. The document allows bare die product to be tested in a surrogate package if the package used is documented.

Failure Criteria (Q100-11 Section 2.9)

This section defines failure as not meeting all device specifications. The section also notes that after CDM testing device parameters can drift from out of specification back into specification. This section encourages post stress testing to be done soon after stress but does not give a time limit.

Acceptance Criteria (Q100-11 Section 2.10)

This section requires that devices classified at a particular level not only has to pass that level of stress but also must pass all lower stress levels.

There are also some slight differences in the classification levels between JS-002 and Q100-11. To account for the 750 V corner pin requirement, AEC has inserted an extra level into their classification

JS-002		Q100-11	
Classification	Description	Classification	Description
C0a	<125	C0a	< 125
C0b	125 to <250	C0b	125 to <250
C1	250 to <500	C1	250 to <500
C2a	500 to <750	C2	500 to < 750
		C2a	500 to <750 (with corner pins ≥ 750)
C2b	750 to <1000	C2b	750 to < 1000
C3	≥1000	C3	1000

Table 1: Comparisons of JS-002 and Q100-11 qualification levels

scheme, creating some confusion. The new Q100-11 level of C2 has the same definition as the JS-002 definition as JS-002 level C2a. To obtain the C2a level in Q100-11 requires corner pins passing 750 V or higher.

SUMMARY

In summary, the ESD requirements for commercial versus automotive qualification are very similar. Both require HBM and CDM testing based on the same two test standards, JS-001 for HBM and JS-002 for CDM. Automotive qualification has additional requirements, including specified qualification target levels, 3 versus 1 zap for CDM, and several additional requirements. The good news is that if a product has met the requirements of AEC Q100 for ESD qualification, the product will more than met the requirements for JEDEC/ESDA qualification for ESD. 

REFERENCES

1. ANSI/ESDA/JEDEC JS-001-2017, “For Electrostatic Discharge Sensitivity Testing, Human Body Model (HBM) – Component Level,” EOS/ESD Association, <https://www.esda.org> and JEDEC Solid State Technology Association, <https://www.jedec.org>.

PRODUCT showcase

2. AEC-Q100-002 REV-E, "Human Body Model Electrostatic Discharge Test," Automotive Electronics Council, <http://www.aecouncil.com>.
3. ANSI/ESDA/JEDEC JS-002-2018, "For Electrostatic Discharge Sensitivity Testing, Charged Device Model (CDM) – Device Level," EOS/ESD Association, <https://www.esda.org>, and JEDEC Solid State Technology Association, <https://www.jedec.org>.
4. AEC-Q100-011 Rev-D, "Charged Device Model (CDM) Electrostatic Discharge (ESD) Test," Automotive Electronics Council, <http://www.aecouncil.com>.

Need Assistance With CE Directives?



Machinery

Low-Voltage

Medical Device

Pressure Equipment

Construction Products

CERTIFI GROUP

Call Us Today 800-422-1651
www.CertifiGroup.com



LIGHTNING EMC

HAEFELY AXOS 8



SURGE

EFT/BURST

VOLTAGE DIPS

MAGNETIC FIELD

RING WAVE

TELECOM

CONTACT:
SALES@LIGHTNINGEMC.COM

HAEFELY
Current and voltage – our passion

IN

COMPLIANCE

Magazine

eNewsletters

Did you know we offer a variety of e-newsletters to help you connect with the EE compliance community?

Personalize your subscription and sign up for the news that matters most to you.

THE WORLD IN COMPLIANCE
A biweekly report on the latest compliance news, standards updates, and more.

PRODUCT INSIGHTS
A monthly exploration of current marketplace products and services, as well as industry events.

TECHCONNECT
Learn from monthly technical white papers, case studies, application notes and more.

[HTTPS://INCOMPLIANCEMAG.COM/ENEWSLETTERS](https://incompliancemag.com/enewsletters)



EXODUS ADVANCED COMMUNICATIONS

EXIT OUT OF THE ORDINARY



COMMERCIAL Applications



EMC Applications



MILITARY Applications

AMP4065B-LC

18.0-26.5GHz,
200W



www.exoduscomm.com

Static

Stop

by SelectTech

The Static Control Flooring Experts

- Maintenance Products
- Most Effective Flooring Solutions
- Industry Leading Technical and Installation Support



www.staticstop.com

877-738-4537

PRODUCT LIABILITY AND YOUR SAFETY LABELS

By Erin Earley

Product safety labels are an important part of keeping users safe and reducing liability risk. There are two main standards for safety labels that are key to creating effective warnings that accurately communicate hazard information: ANSI Z535.4 domestically and ISO 3864-2 internationally. The current versions of these standards allow manufacturers to use different label format options: symbol-only, symbol and text, text-only ANSI, wordless, and multilingual. Deciding the best fit for your intended audience isn't always easy. It helps to understand the product liability and legal landscape. For perspective, we turned to Cal Burnton, a trial attorney with 30 years of experience in product/machinery safety, product liability, and complex litigation. Read our interview below for context on the importance of adequate labels and insight on formatting options, including the increasing trend toward labels that rely mainly or exclusively on symbols.

WHEN IT COMES TO TODAY'S PRODUCT LIABILITY LAWSUITS, HOW IMPORTANT ARE WARNINGS AND PRODUCT SAFETY LABELS?

Warnings and safety labels, along with the manual, should be the most important pieces of evidence in any product liability lawsuit. Exhibit number one should be the warning which, had it been followed, would have prevented the accident. The warnings and labels also put forth a picture of the manufacturer's culture for safety; it's a reflection of the company's concern for the safety of the user. Ultimately the manufacturer wants to be able to show it provided the user with everything necessary to safely use the product. Warnings and instructions give the company the tools it needs to successfully defend a case.

Erin Earley, head of communications at Clarion Safety Systems, shares her company's passion for safer products and workplaces. She's written extensively about best practices for product safety labels and facility safety signs. Clarion is a member of the ANSI Z535 Committee for Safety Signs and Colors, the U.S. ANSI TAG to ISO/TC 145, and the U.S. ANSI TAG to ISO 45001. Erin can be reached at earley@clarionsafety.com.



WHAT TRENDING TOPICS ARE YOU CURRENTLY SEEING IN PRODUCT LIABILITY LAWSUITS THAT INVOLVE INADEQUATE WARNINGS?

Virtually every product liability case has a failure to warn component. The claim is typically simple to make, easy to understand, and often forms the basis for liability. There doesn't even have to be a design or manufacturing defect in the product to lose a failure to warn claim. The claim that "if only the injured party had known" is one most can easily understand. That's why warnings and instructions should be front and center for manufacturers. Warnings can be the downfall of a product but also its salvation.

Many lawsuits involve a misuse of the product. The extent to which the company was able to anticipate foreseeable misuse and therefore warn against it often is a critical issue in a case. Manufacturers must revisit their warnings and instructions regularly to evaluate if they remain adequate, given how the product is being used in the marketplace. Adequacy of warnings will be judged partly by what was known by the company as to the uses and misuse of its product. Companies need to be aware of how their product is being shown on social media. Complaints of injuries must be investigated to determine if a change in warnings is necessary.

Manufacturers will be deemed to be experts in their field, which includes knowing how people are

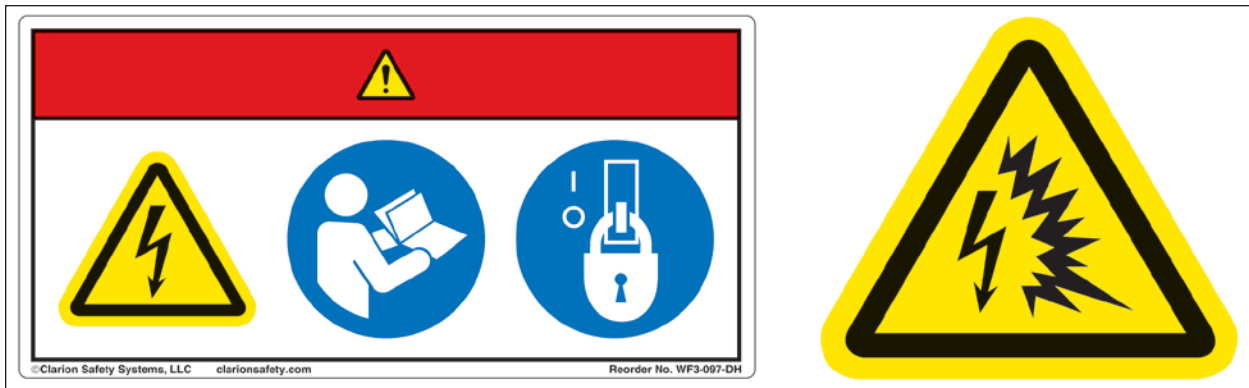


Figure 1: At left, an example of a 'wordless' format safety label and, at right, an example of a 'symbol only' format safety label. These formats meet ISO 3864-2 and are allowed by ANSI Z535 through its section 3.1.1, allowing manufacturers to use ISO formats.

foreseeably using, misusing, and modifying their product. Failure to warn about foreseeable misuses or modifications may lead to liability.

HOW MUCH WEIGHT DO THE ANSI Z535 AND ISO 3864-2 STANDARDS CARRY IN A U.S. COURT OF LAW?

Jurors and judges understand how manufacturers face a variety of difficult issues designing and selling a product. The presence of industry standards such as ANSI Z535 is the starting point for showing that a company made a safe product. If an injured party is able to show that the company failed to meet a standard such as ANSI Z535, defending the case is much more difficult. It will be close to impossible to get dismissed as a defendant prior to trial. But if it can be shown the product meets standards such as ANSI Z535, the company has taken the first steps in defending itself. Meeting a standard doesn't per se establish that a product wasn't defective, but it's a well-recognized piece of evidence that the company acted reasonably and followed established standards in making a safe product. Similarly, ISO 3864-2 can be relied upon by courts, experts, and manufacturers to provide a sound basis to justify that warnings helped to make the product safe to use and non-defective.

IN THE CONTEXT OF PRODUCT LIABILITY LAWSUITS, HOW IMPORTANT IS THE USE OF SYMBOLS IN A WARNING?

The goal of warnings is to adequately communicate a hazard, its severity, and how to avoid the hazard. Warnings serve to inform and remind users of hazards. Often split-second actions are involved

by users of various backgrounds. Hazard symbols have been recognized as having the ability to serve all the needs of an adequate warning. A properly designed symbol can instantly communicate hazards, seriousness, and risk to users from all walks of life, regardless of education and language skills. A symbol in a warning can be easily understood by jurors and judges. Symbols are perhaps the easiest and quickest way to communicate risk to a user.

WHAT'S YOUR LEGAL PERSPECTIVE ON THE 'SYMBOL ONLY' AND 'WORDLESS' APPROACH TO LABELING THAT MEETS ISO 3864-2 (AND IS ALLOWED BY Z535)?

Most important, symbols communicate hazards and how to avoid them. In doing so, they help prevent accidents and, should there be one, give the company tools it needs to defend itself. The goal is to make the product safer and communicate to the user how to safely use the product. Simple symbols should be easy to understand and comprehend. This will lead to fewer accidents, fewer claims, and fewer lawsuits.

Warnings have to do more than warn; they have to adequately warn. So the old method of listing hazards in a laundry list manner, or like a legal contract, will no longer suffice. The warnings must communicate in a simple and direct manner. Pictorials can accomplish just that. The standards recognize that pictorials can communicate messages to users from many walks of life with diverse backgrounds, educational levels, and languages. Manufacturers now have many tools in the tool chest to communicate warnings, and failure to consider a wordless approach would be a mistake. ^{EN}

Banana Skins

404 Household heaters turned on spuriously by interference

The Japanese National Institute of Technology and Evaluation has announced that they have confirmed that some of the household electrical heaters available in Japan malfunction when subjected to electrical disturbances. They conducted the evaluation as a response to the information from consumers that electrical heaters sometimes turned themselves on. They tested thirteen models of heaters for immunity to EFT/B per IEC 61000-4-4. The test results indicated that four of the thirteen samples tested turned themselves on at test level 4 (4kV), and one of them had been caused the malfunction even at test level 1 (0.5kV)!

They also found that two of the thirteen samples could be (unintentionally) controlled by infrared remote controllers for audio/visual products. Fortunately, it seems no fire accidents had been caused – at least at the time of the announcement.

(Sent in by Tomonori ('Tom') Sato, February 2007. Never trust a software-controlled power switch unless it fully complies with all relevant parts IEC 61508. Also see Banana Skin No. 307.)

405 The EM environment in space 200 nautical miles up

The levels of electromagnetic fields that illuminate a satellite, that originate from earth-based sources, now exceed hundreds of volts per meter (V/m). It is pointed out that the electronic circuitry will have to survive these fields and remain operational as well.

MIL-STD-461E (table 1B) requires a space system to be compatible with high external EME levels of 100V/m

from 100MHz-1GHz, but Figure 1 indicates that external fields at 200 nautical miles (nm) height due to earth-based sources such as radio, TV and radars occur out to 100GHz, and up to 250V/m. The field strength at 100 nm will be twice as high.

In a worst-case scenario these sources might cause damage to the on-board electronic devices.

It is also pointed out that EME can be coupled into a system even if it is not operating. Accordingly, a radiated susceptibility test without power applied would be a prudent step to consider.

(Extracted from "Some Simple Spacecraft Considerations," Edward R Heise and Robert E Heise, IEEE 2006 International EMC Symposium, Portland, OR, USA, August 14-18 2006, ISBN: 1-4244-0294-8/06.)

406 Interference problems with the NASA Mars Reconnaissance Orbiter

Because of the selected science experiments, the RF communications link, and the limited space for these elements, the MRO spacecraft had greater than usual EMC considerations. Added to that, the late delivery of some of the hardware prevented early identification and resolution of EMC problems. The problems as identified during the test program are identified as follows:

1. The Electra (UHF) receiver was bothered by: SHARAD transmitting, mostly with ELECTRA uncoded, this was an effect that had not been predicted; MCS with its clock on caused ~8 - 10dB interference; MARCI caused ~3dB interference that had not been predicted.

2. The Shard radar (15-25MHz) was bothered by the C&DH, and its cabling to the power distribution unit and the pyro initiation unit. The basic source was its 24MHz clock, but other frequencies contributed as well.

(Work to resolve these problems was not completely successful in all cases, see the full paper for details - Editor) The spacecraft EMC performance is expected to be adequate for mission needs, but the work to accomplish this status was late, and not as certain as required.

(Extracted from: "The EMC Program for NASA's Mars Reconnaissance Orbiter," Albert Whittlesey et al, IEEE 2006 International EMC Symposium, Portland, OR, USA, August 14-18 2006, ISBN: 1-4244-0294-8/06.)

407 Power quality problems easily solved at bulk mail centre

The New Jersey International & Bulk Mail Center (NJI-BMC), one of the largest United States postal facilities, recently faced a dilemma regarding its six aging 300kVAR capacitor banks in its three load centers. Initially, we explored the possibility of replacing all capacitor banks on the system, because one of the cans overheated and subsequently failed. But the solution was as simple as turning them off.

Seven months ago, one of the six 300kVAR capacitor cans at the facility developed a bulge. Within a month, we replaced it. At that time, our maintenance crew noticed indicating lights on the other capacitor banks were lit. We presumed the remaining five banks would fail, and thought the simplest remedy would be to replace all six at once. An engineer

quoted us approximately \$30,000 for replacement, including labor, material, and testing.

A Surprise Solution. At this point, we realized that lower kVA loads coupled with the existing 300kVAR fixed capacitor banks on each side of the facility had caused the overheating and bulging of the capacitor can. Our preliminary calculation indicated the caps were resonating at 7th and 9th harmonics. After testing this load center, we connected power monitoring meters to all remaining load centers. The data revealed the fixed capacitors (if turned on) were creating higher THDs on the system. Later, we learned these fixed cap banks could also damage our supply transformers and equipment. Our solution was to simply turn the cap banks off. By doing this, we prevented a major transformer failure on our system and avoided lost production time.

(Extracted from "Bulk Mail Center Avoids Transformer Catastrophe," EC&M, Jan 1, 2001, by Dilip Pandya.)

408 Class D amplifier interferes with AM radio

Russ O'Toole, chasing overheating in a Class D power amp hung a scope on the output and found several volts in the MHz range. Not surprisingly, it was wiping out much of the AM broadcast band (MW to our European members). The manufacturer didn't think it was a problem. The FCC did, and shut them down.

(From Jim Brown, on the SC-05-05 mailing list, 7 Dec 2006 15:27:43.)

The regular "Banana Skins" column was published in the EMC Journal, starting in January 1998. Alan E. Hutley, a prominent member of the electronics community, distinguished publisher of the EMC Journal, founder of the EMCIA EMC Industry Association and the EMCUK Exhibition & Conference, has graciously given his permission to republish this reader-favorite column. The Banana Skin columns were compiled by Keith Armstrong, of Cherry Clough Consultants Ltd, from items he found in various publications, and anecdotes and links sent in by the many fans of the column. All of the EMC Journal columns are available at: <https://www.emcstandards.co.uk/emi-stories>, indexed both by application and type of EM disturbance, and new ones have recently begun being added. Keith has also given his permission for these stories to be shared through In Compliance as a service to the worldwide EMC community. We are proud to carry on the tradition of sharing Banana Skins for the purpose of promoting education for EMI/EMC engineers.

409 Rescue robots lose contact due to interference with wireless comms

Plans to send robots equipped with cameras and other sensors into dangerous environments such as burning buildings ahead of human rescue teams could be heading for trouble. More than two-thirds of systems involved in a large-scale trial in the US lost contact with their operators due to radio interference.

Of the 14 types of robot involved in realistic training scenarios, 10 experienced communications problems as a result of interference from other systems. According to the researchers, sticking to industrial, scientific and medical frequency bands designed to minimise interference between different systems is no guarantee of flawless communications between a robot and its operator. (But that's not what the ISM bands are for! – Editor.)

Interference was a problem whenever the frequency being used became crowded or when one user had a much higher output than others. For example, transmitters in the 1760MHz band knocked out 2.4GHz video links, while a robot using an 802.11b signal (colloquially known as Wi-Fi) in the 2.4GHz band overwhelmed and cut off another that had been transmitting an analogue signal at 2.414GHz.

NIST has suggest a number of ways of tackling the problem, including changes in frequency co-ordination, transmission protocols, power output, access priority and using relay transformers to increase the range of

wireless transmissions. (It sounds as if they could also benefit from some good old-fashioned RF design in their hardware, too! – Ed.) In a paper presented at last month's International Symposium on Advanced Radio Technologies in Boulder, Colorado, they also suggest establishing new access schemes of software-defined radios that improve interoperability.

(Extracted from: "Rescue robots hit comms snag," IET Engineering & Technology, April 2007, page 12, <https://www.theiet.org>. This item is also mentioned briefly in New Scientist, 10 March 2007, page 25, <https://www.newscientist.com>. We should worry about this – military and security agencies are keen to use robots to avoid exposing their operatives to risk, and these robots will be armed and even autonomous – able to decide for themselves what to do. See IEEE Spectrum March 2007 page 12, "A Robotic Sentry for Korea's Demilitarized Zone.")

410 ESD interferes with Japanese lifts

On a recent visit to Japan, Dave Imeson, secretary of the very successful and influential EMC Test Laboratories Association, was intrigued to find an electrostatic discharge plate installed near every lift button, with instructions to touch the plate to discharge any electrostatic charge before pressing the button to call the lift.

(Conversation during a break in the IET's "EMC and Functional Safety" Working Group meeting on 9th March 2007, London U.K.) ☺

*The Enhanced
Digital Edition*



Whether you read *In Compliance Magazine* in print or online, we are committed to providing you with the best reading experience possible.

Our enhanced digital edition presents a responsive, interactive, and user-friendly version of the magazine on any device. Check us out online for exclusive bonuses!

[HTTPS://DIGITAL.INCOMPLIANCEMAG.COM](https://digital.incompliancemag.com)

Advertiser Index

A.H. Systems, Inc.	Cover 2
AR	3
CertifiGroup	23, 45
Coilcraft	15
E. D. & D., Inc.	7
ETS-Lindgren	Cover 4
Exodus Advanced Communications	45
HV TECHNOLOGIES, Inc.	11
Kikusui America	25
Lightning EMC	45
Raymond EMC	33
StaticStop by SelecTech	45
Suzhou 3ctest Electronic Co. Ltd.	19

Upcoming Events

November 1-4

Applying Practical EMI Design & Troubleshooting Techniques

Advanced Printed Circuit Board Design for EMC + SI

Mechanical Design for EMC

November 7-11

EMC Week

Visit incompliancemag.com/EERC
to access your free resources today!



SELECTING RF MICROWAVE POWER AMPLIFIERS FOR EMC TESTING

application note provided by



GUIDE TO NON-CONTACT SENSORS AND THEIR APPLICATIONS

application note provided by



UNDERSTANDING REACH ON A GLOBAL SCALE

white paper provided by



BASICS OF LEAKAGE CURRENT TESTING

video provided by



ANTENNA BEAMWIDTH COVERAGE CALCULATIONS

calculator provided by



DEFINITIVE GUIDE FOR DO-160G SECTION 16.0: POWER INPUT

white paper provided by



CAN ELECTROMAGNETIC COMPATIBILITY AND ANTENNA MEASUREMENT TESTING BE PERFORMED IN THE SAME CHAMBER?

video provided by



GLOBAL CERTIFICATION FOR PRODUCTS WITH WIRELESS FUNCTIONS

white paper provided by





SERVICES BEYOND MEASURE.

From education to consulting, product testing to calibration, ETS-Lindgren has more than 800 dedicated experts, and over 60 independent representatives around the globe committed to the success of our customers— whether in Asia, Europe, the Middle East, or the Americas.

ETS-Lindgren's world class excellence refers not only to talent, but to our state-of-the-art offerings that include a NVLAP accredited test lab (NVLAP Lab Code 100286-0), CTIA Authorized Test Lab (CATL), and our 2017 designation as the first, and only, MIMO/OTA CTIA Authorized Equipment List supplier. Stay on track with development and production, and protect your assets with ETS-Lindgren's suite of specialized Services and Support that include:

- Calibration & Repair
- Engineering & Consulting
- Field Services & Site Surveys
- Maintenance & Upgrades *featuring Calibration Service Plus!™*
- Acoustic, Wireless & EMC Product Testing *with TILE!™ and EMQuest!™*
- Site Planning & Design *with BIM Technology*
- Training & Education *with ETS-U™*

For more information on ETS-Lindgren Services, visit our website at www.ets-lindgren.com.

Connect with us at:



BEYOND MEASURE.™

ETS·LINDGREN
An ESCO Technologies Company

Offices Worldwide | ets-lindgren.com

11/22 RR © 2022 ETS-Lindgren v1.0